

Reproduction of Ross' linear-mixing model for the equation of state of deuterium

Jason W. Bates*

Laser Plasma Branch, Plasma Physics Division

U.S. Naval Research Laboratory, Washington, DC 20375 USA

(Dated: February 4, 2002)

Abstract

The linear mixing (LM) model proposed by Ross [Phys. Rev. B **58**, 669 (1998)] can accurately reproduce experimental Hugoniot data for shocked liquid deuterium at pressures up to 6 Mbar. Using a simple dissociation scheme, the model smoothly interpolates between (or linearly “mixes”) a molecular fluid equation of state (EOS) applicable at low pressures, and a metallic-like description valid at high densities, with the relative composition of the mixture determined by minimizing the total Helmholtz free energy of the system. Although the formulation of the LM model is straightforward, it nevertheless involves a series of nontrivial computations and results whose details are fragmented in the published literature. In this report, we present an explicit and self-contained reproduction of the LM model, and correct minor typographical errors that appeared in the original publications. Limitations of Ross' approach and comparisons with popular alternate theories are also discussed, although no attempt is made to conduct a thorough survey of existing EOS models for deuterium. Listings of the Mathematica codes used to compute the principal Hugoniot curve, and equilibrium thermodynamic quantities such as the specific heat, Grüneisen coefficient, and sound speed, are provided in the appendices.

PACS numbers: 64.30+t,52.50.Lp,51.35.+a

Keywords: Deuterium, equation of state, linear mixing model

*bates@this.nrl.navy.mil

I. INTRODUCTION

Inertial confinement fusion (ICF) is perhaps the most promising approach to realizing controlled power production from thermonuclear fusion reactions. In the archetypal ICF scheme, microcapsules containing isotopes of hydrogen are compressed by a series of strong shock waves generated by intense radiation [1]. The design of these microcapsules, though, relies heavily on hydrodynamic-based computer codes to realistically simulate the compression process. Knowledge of the compressibility of hydrogen at high density and temperature is thus paramount for the fidelity of ICF simulations. In addition, an understanding of the thermodynamic properties of hydrogen at extreme conditions is a requirement for modeling planetary and stellar structures such as Jovian planets [2, 3] and brown dwarfs [4].

The compressibility of matter over a wide range of conditions is embodied in the equation of state (EOS), which usually is a functional statement of how the pressure and specific internal energy of a substance depend on density and temperature [5]. Although it is the simplest of all elements, hydrogen has poorly understood EOS properties, particularly above pressures of 0.5 Mbar where it is expected to undergo a phase transition from a molecular to a metallic state [6–9]. Moreover, since hydrogen is usually diatomic at low temperatures, other physical processes such as rotation, vibration, and dissociation pose additional phenomenological challenges to developing a realistic, wide-ranging EOS theory.

In most theoretical studies of the EOS properties of hydrogen, deuterium has been the preferred isotope to consider because of its direct application to fusion studies. In addition, the higher atomic mass of deuterium usually corresponds to higher experimental pressures and densities, which is advantageous because it permits lower uncertainties in the data used to benchmark the theory [10]. Tritium, of course, possesses even greater atomic mass than deuterium, but the associated radiation hazard [11] usually outweighs any gain in experimental accuracy that this isotope may offer. Furthermore, it is often assumed that EOS results for deuterium may be scaled to apply to hydrogen or tritium without introducing significant errors [12–14].

Traditionally, the most useful class of experiments for probing the EOS properties of materials such as deuterium at extreme conditions involves the use of strong shock waves [15, 16]. Although methods employing diamond-anvil cells [17] have achieved pressures in excess of 1 Mbar [18], they have a fundamental disadvantage in that they do so close to room

temperature. Present shock-based methods, on the other hand, can reach temperatures corresponding to several electron-volts, which is more relevant for ICF and astrophysical studies [19]. Different methods exist for producing strong shock waves, including the detonation of high explosives [20], the impact of high-speed projectiles propelled by gas-guns [21], or the absorption of an intense radiation pulse from a high-powered laser on a dense target [22].

Sophisticated optical and electronic techniques are normally required to determine the shock and particle velocities, which along with a knowledge of the initial state, can then be used to compute the final density, pressure, and energy according to the Rankine-Hugoniot relations [23]. For planar shock waves, these relations are

$$V_0/V = \rho/\rho_0 = D/(D - u) , \quad (1)$$

$$p - p_0 = \rho_0 D u , \quad (2)$$

$$\varepsilon - \varepsilon_0 + u^2/2 = pu/(\rho_0 D) . \quad (3)$$

Here, V is the specific volume, $\rho = 1/V$ is the density, p is the pressure, and ε is the internal energy per unit mass. The variables D and u denote the shock and downstream particle velocities, respectively, in the laboratory frame of reference. Subscripts “0” refer to the undisturbed state ahead of the shock, which is assumed to be in thermodynamic equilibrium. The Rankine-Hugoniot relations are a statement of the conservation of mass, momentum, and energy across a discontinuity, and are derived under the assumptions that local thermodynamic equilibrium exists immediately behind and in front of the shock, and that the material possesses negligible material strength [15]. Equations (1)-(3) can be combined into a single relation involving the thermodynamic variables only. This is known as the Hugoniot equation, and is given by

$$\varepsilon - \varepsilon_0 = \frac{1}{2}(p + p_0)(V_0 - V) . \quad (4)$$

If ε is known as a function of V and p , then Eq. (4) defines the principal Hugoniot curve, which plays an important role in the study of shock waves and the EOS properties of materials. This curve is the locus of all possible states that may be reached by a single shock, starting from some initial values of density and pressure, and leading to a pair of “shocked” values [24]. Note that the temperature is not obtained directly from the Hugoniot

equation. Although it can be measured if the optical emission from the shock is sufficiently high, it is usually obtained from a theoretical EOS model [15].

For deuterium, results from recent, laser-driven shock experiments performed at Lawrence Livermore National Laboratory [25, 26], and at the U.S. Naval Research Laboratory [27, 28], have cast doubt on popular EOS models used extensively in the past. In the Livermore experiments, high-energy laser pulses were employed to generate principal Hugoniot data points at pressures up to ~ 3 Mbar, and densities in the neighborhood of 1 g/cm^3 , corresponding to a maximum compression ratio of the deuterium target of about 6. This value is about 50% greater than predicted from the widely-used, Sesame EOS database [29, 30]. Furthermore, other models based on pairwise additive intermolecular potentials [31–33] that had been very successful in explaining earlier, low-pressure gas-gun experiments [34–36], also showed poor agreement with the new data when attempts were made to extend these theories to the high-pressure regime. The same problem has held true for sophisticated simulation techniques such as path-integral Monte Carlo (PIMC) methods [37–39], and *ab initio* molecular dynamics (MD) calculations [40–43], and has raised the question as to whether non-equilibrium and/or non-planar shock effects may play a role in explaining the discrepancy.

A straightforward equilibrium theory that has succeeded in accurately reproducing the new high-pressure Hugoniot data for deuterium is the so-called linear-mixing (LM) model proposed by Ross [34, 44]. The LM model employs two distinct equations of state: one to describe a low-pressure molecular fluid, and another for a high-density monatomic-metallic fluid. The molecular EOS is formulated using a variational hard-sphere theory with soft-sphere corrections [45–49], while the metallic EOS relies on a one component plasma (OCP) methodology [50, 51], including degenerate electrons. An ideal mixing scheme is employed for conditions in which both fluid states are present. The mixing parameter, which is equivalent to the degree of dissociation in the fluid, is determined by minimizing the total Helmholtz free energy of the system. The model thus has the practical advantage that it smoothly interpolates between two well-established equations of state that are build into the description as limiting cases. At very high temperatures and pressures, when the thermal energy is comparable to, or exceeds, the Fermi energy of the metallic state, deuterium is a dense partially-ionized plasma of atoms, ions, and electrons, whose characterization lies outside the scope of the LM model. In that case, other models such as ACTEX [52, 53] likely provide a better description of the physics. In this report, though, our attention is limited

to the LM model, an explicit and self-contained reproduction of which is our principal task.

The success of the LM model seems to depend strongly on its treatment of the dissociation process. While the Sesame EOS database and the PIMC and MD calculations cited earlier all include dissociation at some level of approximation, it is apparently not sufficient to reproduce the high-pressure experimental data very well. The enhanced dissociation — and concomitant higher compressibility — displayed by the LM model is undoubtedly due in part to the use of a large entropy shift in the Helmholtz free energy of the metallic state of approximately 3 eV per atom (at the thermodynamic conditions near the peak compression of the principal Hugoniot), which Ross introduces as a crude estimate of electron screening effects [44], and/or the presence of chainlike structures [54] omitted by the LM model. This term does not affect the pressure or specific internal energy directly, but it does influence the degree of dissociation significantly. We should mention, though, that Arnault *et al.* [55] have reported that electron screening effects alone are not enough to explain all the experimental data. Zinamon and Rosenfeld [56] have pointed towards a different physical mechanism (also omitted entirely by the LM model) that could account for the enhanced compressibility without use of this entropy shift: thermal electron-correlation effects. These issues and others have raised some controversy in the ICF community about the LM model, but we shall not attempt to resolve them in this report. Rather, we mention them here as a matter of record, and shall limit our attention to reproducing Ross' LM model in its simplest form.

The organization of this report is as follows. In Sec. II, we provide a detailed formulation of the LM model, and correct minor typographical errors that appeared in the original presentation. In Sec. III, we use this model to generate the principal and secondary Hugoniot curves for deuterium, and show that they agree well with most experimental data. In addition, we also compute the variation of various equilibrium thermodynamic quantities along the principal Hugoniot, including the specific heat, Grüneisen coefficient, and sound speed. Section IV provides a summary of the results. Finally, the appendices contain listings of the actual Mathematica codes used in this investigation, along with examples of their output. The use of a computational platform with symbolic manipulation capabilities such as Mathematica [57] was particularly useful in this study because of the ease with which certain quantities such as derivatives, integrals, residues, interpolated functions, and roots of equations could be calculated accurately and easily. Throughout this report, an attempt

is made to express all physical quantities in terms of Gaussian cgs units, although at times, exceptions are made when it is convenient to do so. Examples of such exceptions include the use of Mbar and eV units for expressing pressures and temperatures, respectively.

II. STRUCTURE OF THE LM MODEL

At the crux of the LM model is an assumption that the thermodynamic properties of a dissociating diatomic fluid can be described as a weighted mixture of molecular and monatomic equations of state. This approach builds in the correct limiting behavior at low and high densities, and uses the fraction of dissociated molecules, x , as a interpolation parameter to find the properties of intermediate states. The total Helmholtz free energy F of the system is written as

$$F(x, \rho, T) = (1 - x) F_{D_2}(\rho, T) + x F_D(\rho, T) - T S_{mix}(x) , \quad (5)$$

where F_{D_2} and F_D are the Helmholtz free energies per unit mass of the pure molecular and monatomic fluids, respectively. The entropy of mixing, S_{mix} , is given by

$$S_{mix} = -Nk \left[(1 - x) \ln \frac{1 - x}{1 + x} + 2x \ln \frac{2x}{1 + x} \right] , \quad (6)$$

where N is the number of molecules (or equivalently, pairs of atoms) per unit mass, and k is Boltzmann's constant. (See Table I for a listing of the physical constants relevant to this study.) The dissociation fraction x , which is treated as an independent variable in F , is found from minimizing the right side of Eq. (5). The result is

$$\frac{x^2}{1 - x^2} = \exp [-(F_D - F_{D_2})/NkT] \equiv q(\rho, T) , \quad (7)$$

or

$$x = \sqrt{\frac{q}{4 + q}} . \quad (8)$$

Once F_D and F_{D_2} are known as functions of ρ and T , the dissociation fraction is uniquely determined. Strickly speaking, Eq. (6) is a correct expression for the entropy of mixing only in the limit of an ideal, dissociating diatomic gas in which the independent thermodynamic variables are actually pressure and temperature, and not density and temperature, as we have assumed here [58]. In the present calculation, one could argue that the entropy of mixing is more correctly given by [29]

$$S_{mix} = -Nk [(1 - x) \ln(1 - x) + 2x \ln x] , \quad (9)$$

which upon minimizing Eq.(5), gives instead

$$\frac{e x^2}{1-x} = q(\rho, T), \quad (10)$$

where e is the base of the natural logarithm. Solving Eq. (10) for x yields

$$x = \frac{q}{2e} \left(\sqrt{1 + 4e/q} - 1 \right). \quad (11)$$

In Eq. (11) we have used the fact that x is positive and varies between zero and one. In practice, however, it turns out that the features of the Hugoniot curve are not strongly affected by this correction. That is, either Eq. (8) or Eq. (11) may be used to calculate the dissociation fraction, with essentially the same result being obtained in both cases.

Expressions for the pressure and specific internal energy are computed by taking appropriate derivatives of the Helmholtz free energy [59], and are given by

$$p = \rho^2 \frac{\partial F}{\partial \rho} = (1-x) p_{D_2} + x p_D, \quad (12)$$

$$\varepsilon = -T^2 \frac{\partial}{\partial T} \left(\frac{F}{T} \right) = (1-x) \varepsilon_{D_2} + x \varepsilon_D. \quad (13)$$

Note that any constant term that appears in F must also appear in ε , but the same is not true for an entropic term (*i.e.*, $F \sim NkT$). Let us now turn to a summary of the EOS calculations for the molecular and monatomic fluid phases.

A. Molecular EOS

At moderately high densities ($0.2 \text{ g/cm}^3 \lesssim \rho \lesssim 0.5 \text{ g/cm}^3$), but relatively low temperatures ($T \lesssim 4000 \text{ K}$) and pressures ($p \lesssim 0.2 \text{ Mbar}$), deuterium is a molecular fluid [10]. The thermodynamic properties of this fluid can be well characterized by writing down a superposition of several free-energy terms that model various kinetic processes occurring in the molecular phase. Such processes include translational, rotational, and vibrational motion, as well as the effects of attractive and repulsive forces between molecules. In the LM model, the Helmholtz free energy of the diatomic phase of liquid deuterium is written as

$$F_{D_2}(\rho, T) = F_{D_2}^0(\rho, T) + F_{int}(T) + F_{con}(\rho, T) + ND_0 + 2NE_0, \quad (14)$$

where D_0 is the well depth of the diatomic potential (the negative of the dissociation energy of the deuterium molecule), and E_0 is the binding energy of an electron in a deuterium

atom; see Table I for numerical values. The functions $F_{D_2}^0$, F_{int} , and F_{con} are known as the translational, internal, and configuration free energies, respectively.

The translational free energy, $F_{D_2}^0$, accounts for the kinetic energy of motion of the deuterium molecules. Assuming ideal gas behavior, it is given by [60]

$$F_{D_2}^0 = -NkT \left[\ln \frac{(2\pi m_{D_2} kT)^{3/2}}{N\rho h^3} + 1 \right], \quad (15)$$

where m_{D_2} is the mass of a deuterium molecule, and h is Planck's constant. The second term in Eq. (14), which represents the contribution to the free energy from internal vibrational and rotational motion of the diatomic molecule, can be approximated as [23]

$$F_{int} = -NkT \ln \frac{Z_\nu T}{2\theta_{rot}}, \quad (16)$$

where Z_ν is the partition function associated with vibrational motion of the diatomic molecule, and $\theta_{rot} = \hbar^2/(2kI_{D_2})$ is a characteristic rotational temperature for deuterium; here, the symbol \hbar denotes Planck's constant h divided by 2π , and I_{D_2} is the moment of inertia of a diatomic deuterium molecule. Using a harmonic oscillator potential to approximate the vibrational energy states (including the zero-point energy contribution), we can write [5]

$$Z_\nu(T) = \frac{e^{-\theta_{vib}/2T}}{1 - e^{-\theta_{vib}/T}}. \quad (17)$$

In this expression, the quantity $\theta_{vib} = h\nu_{D_2}/k$ is a characteristic vibrational temperature for the deuterium molecule, and ν_{D_2} is the vibrational frequency. Note that in this description, contributions to the molecular free energy from excited electron states are neglected. Also note that Z_ν is unbounded as $T \rightarrow \infty$, which can lead to unphysical behavior in the dissociation fraction for some simple EOS models of diatomic fluids [61]. For the LM model, though, the function Z_ν appearing in Eq. (17) causes no such difficulty and shall be adopted throughout this report.

The term F_{con} in Eq. (14) is the configurational free energy, and represents the contribution from potential interactions between molecules within the deuterium fluid. Using a hard-sphere variational theory with a soft-sphere correction, and ignoring effects associated with the asymmetry of diatomic molecules (*i.e.*, assuming complete isotropy), Ross, Rhee, and Young [49] derived the following expression for the configurational free energy:

$$F_{con} = \left[\left\{ \frac{4\eta - 3\eta^2}{(1 - \eta)^2} - (\eta^4/2 + \eta^2 + \eta/2) \right\} NkT + I \right]_{d=d_{min}}, \quad (18)$$

where

$$I(\rho, d) = \frac{\rho N}{2 m_{D_2}} \int_d^\infty 4\pi r^2 \phi(r) g_{HS}(r/d, \eta) dr. \quad (19)$$

Here, the dimensionless quantity

$$\eta(\rho, d) = \frac{\pi \rho d^3}{6 m_{D_2}}, \quad (20)$$

is the close-packing fraction for spheres, and d is a variational parameter known as the hard-sphere diameter; for a given density and temperature, it is evaluated at d_{min} , which is the value of d that *minimizes* F_{con} . The expression involving the curly brackets on the right side of Eq. (18) is the free energy of the hard-sphere reference system, and is a combination of two terms: the configurational free energy for a fluid with simple hard-sphere interactions [62], $(4\eta - 3\eta^2)/(1 - \eta)^2 NkT$, and a somewhat *ad-hoc* factor $(\eta^4/2 + \eta^2 + \eta/2) NkT$, which has been subtracted from this expression to yield a result that is more consistent with a softer, “inverse-twelfth-power” repulsion, and is in better agreement with computer simulation data [48] for a wider range of molecular interaction potentials, $\phi(r)$. The term I in Eq. (18) represents the soft-sphere correction in the fluid variational theory [49], and is a spatial integral over the radial variable r of the potential ϕ with g_{HS} , the pair distribution function for hard spheres. Let us now turn to a discussion of how ϕ and g_{HS} are computed in the LM model.

An accurate analytical expression for the effective pair potential ϕ has been determined empirically from early shock-wave data [35] on the EOS of deuterium up to 0.76 Mbar. Using this potential, Ross, Ree, and Young [49] were able to successfully predict fluid and solid isotherms, melting curves, and even a metallic transition pressure, although the exact value of the latter is still somewhat in question [63]. The function ϕ is a slightly modified version of the so-called Silvera-Goldman (SG) potential [64]:

$$\phi_{SG}(r) = \exp(\alpha - \beta r - \gamma r^2) - \left(\frac{c_6}{r^6} + \frac{c_8}{r^8} - \frac{c_9}{r^9} + \frac{c_{10}}{r^{10}} \right) f_{SG}(r), \quad (21)$$

where α , β , γ , c_6 , c_8 , c_9 , and c_{10} are all constant parameters. The function f_{SG} is given by

$$f_{SG}(r) = \begin{cases} 1 & \text{if } r \geq r_0, \\ \exp[-(r_0/r - 1)^2] & \text{if } r < r_0, \end{cases} \quad (22)$$

where r_0 is a constant. As written, the SG potential is expressed in terms of the atomic energy units of hartree, where

$$1 \text{ hartree} = 4.360 \times 10^{-11} \text{ erg}.$$

Thus, Eq. (21) must be multiplied by the conversion factor 4.360×10^{-11} erg/hartree to be expressed in the desired energy units of erg. Note that all the constants in Eqs. (21) and (22) have been adjusted so that the radial coordinate r here is understood to have units of Angstroms (\AA), and not the atomic units of bohr radii, as was the case in Ref. [49].

Although by itself the SG potential can reproduce the static compression data of deuterium at 75-300 K to 0.02 Mbar rather well [65, 66], it fails to explain the static [67, 68] and dynamic [35, 48, 69, 70] data at higher pressure. Ross, Rhee, and Young found, though, that by “softening” the SG potential for values of r smaller than a critical value r_c , better overall agreement with experimental data could be obtained [49]. The result is the potential ϕ that is used to compute the soft-sphere correction term in LM model; it is given by

$$\phi(r) = \begin{cases} \phi_{SG}(r) & \text{if } r \geq r_c, \\ \phi_{SG}(r_c) \exp[-c_1(r - r_c) - c_2(r - r_c)^2 \\ -c_3(r - r_c)^3 - c_4(r - r_c)^3(r - r_1)] & \text{if } r < r_c, \end{cases} \quad (23)$$

where $c_1 \dots c_4$ and r_1 are constants. The 14 parameters needed to compute ϕ are listed in Table II. A plot of ϕ is shown in Fig. 1.

Next, we need to determine an expression for the pair distribution function for hard spheres, g_{HS} . A convenient representation of this function was reported by Wertheim [71], who found a closed-form solution to the Percus-Yevick equation [72]. The results can be summarized as follows. With the abbreviation $x = r/d$, the expression for g_{HS} is given by

$$g_{HS}(x, \eta) = \sum_{n=1}^{\infty} g_{HS}^{(n)}(x, \eta), \quad (24)$$

where

$$g_{HS}^{(n)}(x, \eta) = \begin{cases} 0 & \text{if } x < n, \\ (12\eta x)^{-1} \sum_{\ell=0}^2 \text{Res} [e^{t\ell(x-n)} \{L(t_\ell, \eta)/S(t_\ell, \eta)\}^n t_\ell] & \text{if } x > n. \end{cases} \quad (25)$$

Note that in Eq. (25), the symbol *Res* stands for *residue*, and the functions L and S are polynomials in the dummy variable t :

$$L(t, \eta) = 12\eta[(1 + \eta/2)t + 2\eta + 1], \quad (26)$$

$$S(t, \eta) = (1 - \eta)^2 t^3 + 6\eta(1 - \eta)t^2 + 18\eta^2 t - 12\eta(1 + 2\eta). \quad (27)$$

The three roots of S , which are required for the evaluation of Eq. (25), are

$$t_\ell = 2\eta(1-\eta)^{-1} \left[-1 + x_+ e^{2\ell\pi i/3} + x_- e^{-2\ell\pi i/3} \right], \quad \ell = 0, 1, 2 \quad (28)$$

where

$$x_\pm = \pm \left[\pm f + \sqrt{f^2 + 1/8} \right]^{1/3}, \quad (29)$$

and $f(\eta) = (3 + 3\eta - \eta^2)/(4\eta^2)$. Note that a typographical error that appeared in the expression for x_\pm originally given by Wertheim in Ref. [71] has been corrected in Eq. (29). Also note that in Eq. (28), the symbol i denotes $(-1)^{1/2}$. A plot of g_{HS} for three different values of η is shown in Fig. 2.

We should remark about the physical interpretation of the pair distribution function g_{HS} . Essentially, this function provides an answer to the following question [72]: If we know that there is a particle (deuterium molecule) at the origin $r = 0$, is it more or less likely *than average* that another particle (molecule) will be found at position r ? With this in mind, the significance of several features of Fig. 2 become apparent; these include a region for $r < d$ where $g_{HS} = 0$ due to the hard-sphere repulsion of other molecules by the one at the origin, a large “bump” representing a shell of neighbors in the attractive part of the central molecule’s potential, and a few higher-order “wiggles” due to the presence of additional molecules surrounding this shell. Note that asymptotically, g_{HS} approaches unity at large distances, which represents its “average” value. For an ideal gas, the pair distribution function is everywhere unity since interactions are absent, and a single particle cannot influence the distribution of its neighbors in any way.

Using the expressions for ϕ and g_{HS} in Eqs. (23) and (24), the integral I in Eq. (19) can be evaluated numerically as a function of ρ and d . In the present study, where we are primarily interested in computing the principal Hugoniot for deuterium, the range of interest for these parameters is $\sim 0.4 - 1.2$ g/cm³, and $\sim 0.9 - 1.8$ Å, respectively. A Mathematica computer code to perform this calculation is listed in Appendix A. In addition to I , the code also evaluates the integral expression

$$I_\eta = \frac{\rho N}{2 m_{D_2}} \int_d^\infty 4\pi r^2 \phi \frac{\partial g_{HS}}{\partial \eta} dr, \quad (30)$$

which is required to compute the derivative of F_{D_2} with respect to ρ , and hence the pressure of the molecular fluid [see Eq. (12)]. In terms of I and I_η , the expression for the pressure

and the specific internal energy of the molecular fluid phase are

$$p_{D_2}(\rho, T) = \rho N k T + \left[2\eta \left\{ \frac{2 - \eta}{(1 - \eta)^3} - \eta^3 - \eta - \frac{1}{4} \right\} \rho N k T + \rho I + \rho \eta I_\eta \right]_{d=d_{min}}, \quad (31)$$

$$\varepsilon_{D_2}(\rho, T) = \left[\frac{5}{2} + \frac{\theta_{vib}}{2T} + \frac{\theta_{vib}/T}{e^{\theta_{vib}/T} - 1} \right] N k T + I|_{d=d_{min}} + N D_0 + 2N E_0. \quad (32)$$

Repeated evaluation of I for a series of ρ and d values permits the construction of an interpolation table for determining d_{min} , which we shall say more about in connection with the Hugoniot calculation in Sec. III. An example of the output from the code in Appendix A is provided in Appendix B.

B. Metallic EOS

In this section, we describe the model adopted by Ross for characterizing the monoatomic phase of liquid deuterium at high pressures ($p \gtrsim 0.2$ Mbar). The approach relies on concepts borrowed from the theory of liquid metals [73], and employs a metallic EOS to approximate the properties of the monoatomic fluid. The metallic EOS combines a density-dependent, nearly-free-electron gas description [74] with a modified one-component-plasma (OCP) model [50]. The complete expression for the Helmholtz free energy of the metallic phase is written

$$F_D(\rho, T) = F_D^0(\rho, T) + F_{EG}(\rho) + f_{LDA}(\rho) + F_{OCP}(\rho, T) + 2N\delta_e k T, \quad (33)$$

where δ_e is a constant. Let us now identify and discuss the significance of each term on the right side of Eq. (33).

The first term, F_D^0 , is the free energy associated with translational motion of the deuterium ions. It is given by [60]

$$F_D^0 = -2N k T \left[\ln \frac{(2\pi m_D k T)^{3/2}}{2N \rho h^3} + 1 \right], \quad (34)$$

where m_D denotes the mass of a deuterium ion. Note that this expression is identical to the Helmholtz free energy of a monatomic ideal gas with $2N$ particles per unit mass.

The second term on the right side of Eq. (33) represents the free energy of an electron gas (EG) that immerses a lattice of positive ions. In the LM model, it is approximated as

$$F_{EG} = 2N \left[\frac{2.21}{(r_s/a_0)^2} - \frac{0.916}{r_s/a_0} - \frac{0.88}{r_s/a_0 + 7.8} - \frac{1.792}{r_s/a_0} \right]. \quad (35)$$

In condensed matter theory, the four terms on the right side of Eq. (35) are often referred to as the kinetic, exchange, correlation, and Madelung energies, respectively [74]. The quantity a_0 in Eq. (35) is the Bohr radius, and r_s is the density-dependent ion-sphere radius, which is given by

$$r_s(\rho) = \left[\frac{3A_D}{4\pi N Z_D \rho} \right]^{1/3}. \quad (36)$$

Here, the parameters A_D and Z_D denote the mass number and atomic number, respectively, of deuterium. Note that as written, Eq. (35) is expressed in units of Ry/g, where the symbol Ry stands for *Rydberg* and $1 \text{ Ry} = 13.60 \text{ eV}$. For our purposes, it is desirable to convert F_{EG} to the Gaussian cgs units of erg/g; this requires multiplying Eq. (35) by a factor

$$13.60 \text{ eV/Ry} \times 1.602 \times 10^{-12} \text{ erg/eV} = 2.179 \times 10^{-11} \text{ erg/Ry}.$$

The density-dependent term f_{LDA} in Eq. (33) is equivalent to the Hartree energy in the pseudo-potential theory of metals [34]. In the LM model, this term purportedly corrects for screening and band-structure effects that are omitted by the simple free-electron-gas model [44]. Previous total-energy calculations [75] for metallic hydrogen using a local density approximation (LDA) suggest that f_{LDA} is well represented by the simple analytical expression

$$f_{LDA} = 2N \left[-0.11382 + 0.003554 r_s/a_0 - 0.012707 (r_s/a_0)^2 \right]. \quad (37)$$

The units of Eq. (37) are Ry/g, and thus multiplication by the factor $2.179 \times 10^{-11} \text{ erg/Ry}$ is required to cast this expression in Gaussian cgs units.

The penultimate term in Eq. (33) is the thermal free energy of a OCP in which positive ions are immersed in a constant-density background of fully-degenerate electrons. In the OCP description [51], electron-ion screening and other nonideal effects are ignored. This model is believed to be exact in the limit of extremely high densities. Slattery, Doolen, and DeWitt [50] have determined the thermal free energy of the OCP fluid by exhaustive computer simulation, with an excellent fit to the results being given by

$$F_{OCP} = 2NkT \left[4 \left(d_1 \Gamma^{1/4} - d_2 \Gamma^{-1/4} \right) + d_3 \ln \Gamma - d_4 \right], \quad (38)$$

where $d_1 = 0.95280$, $d_2 = 0.18907$, $d_3 = -0.81773$, and $d_4 = 2.59$ are constants. We should point out that the coefficient d_4 differs in sign from the value reported by Holmes, Nellis, and Ross [34]; the latter was apparently a typographical error. The function Γ in Eq. (38)

is known as the coupling parameter in OCP theory, and is the ratio of potential to thermal energies:

$$\Gamma(\rho, T) = \frac{(Z_D e)^2}{r_s kT}. \quad (39)$$

Here, the symbol e represents the electronic charge and not the base of the natural logarithm.

The final quantity on the right side of Eq. (33), $2\delta_e NkT$, is an entropic term that is added to the metallic free energy in the LM model in its simplest form to account (ostensibly) for higher-order corrections due to electron-ion screening effects. According to Ross [44], the constant δ_e has been determined from a fit to reflected shock temperatures measured in gas-gun experiments [34, 35], and has a nominal value of -2.8 .

III. RESULTS AND DISCUSSION

In the previous section, we outlined the scope and methodology of Ross' approach for modeling the EOS of deuterium. In addition, we presented explicit phenomenological expressions for each of the physical processes that are thought to make significant contributions to the Helmholtz free energy in the molecular and metallic fluid phases. Here, our intent is to demonstrate how the LM model can be used to calculate Hugoniot curves for shock-compressed liquid deuterium, as well as various thermodynamic quantities such as the specific heat, Grüneisen coefficient, and equilibrium sound speed. Let us now describe how this is accomplished.

In general, the principal task required for calculating the principal Hugoniot curve for any EOS model is the solution of Eq. (4). Given that we have expressions for the specific internal energy $\varepsilon(\rho, T)$ and pressure $p(\rho, T)$ that can be substituted into Eq. (4) — and the initial data ρ_0 , T_0 , p_0 , and ε_0 are also known — the solution strategy usually proceeds as follows. First, a particular value of temperature $T > T_0$ is specified. Next, Eq. (4) is solved numerically for the value of ρ that corresponds to this temperature along the Hugoniot using a nonlinear iterative scheme such as Newton's method [76]. The procedure can then be repeated for a sequence of temperature values, and in the way a Hugoniot curve can be generated in, say, the plane of pressure versus density. Note that it is highly preferable to choose the temperature — and not the density — as the parametric variable, since the Hugoniot is not always a monotonic function of the latter.

For the LM model, the procedure outlined above is slightly more complicated because the Hugoniot equation must be solved subject to the constraint that the configurational free energy F_{con} be minimized. For each specified value of temperature, we now must compute self-consistently the values of two parameters: ρ and d_{min} . These parameters must simultaneously satisfy Eq. (4), and an equation that ensures the minimization of F_{con} . In the LM model, the latter equation is derived from setting the derivative with respect to d of the right side of Eq. (18) equal to zero. [Strictly speaking, one should also consider the variation of Eq. (18) with respect to density, but this is usually a less important effect, and is neglected here.]

Before the differentiation of Eq. (18) can be performed, however, the integral expression I in Eq. (19) must be known as a function of ρ and d . For this purpose, the table listed in Appendix B is particularly useful. In the reproduction of the LM model described in this report, two-dimensional cubic polynomials were used to interpolate smoothly the function I over the discrete set of tabulated ρ and d values. The derivative with respect to d of this interpolation function could then be computed easily, and used to simultaneously solve for the values ρ and d_{min} in the Hugoniot calculation. A Mathematica code that executes this dual root-finding procedure is presented in Appendix C; output data from the code appear in Appendix D.

The principal Hugoniot curve for deuterium calculated with the LM model is shown in Fig. 3. For comparison, data from gas-gun [34–36] and Nova laser experiments [25, 26], as well as the deuterium Hugoniot derived from other theoretical EOS models are also shown. These include the Sesame database [29], and so-called “tight-binding” [40] and “generalized gradient approximation” [41] methods, which are different classes of molecular dynamics calculations and are abbreviated here as TBMD and GGA-MD, respectively. Near the initial state where $x \simeq 0$, the Hugoniot for the LM model at first tracks quite closely the result computed with the molecular EOS alone (the short dashed line in Fig. 3), as one would expect, but as the pressure and dissociation fraction rise, it departs significantly from the molecular EOS limit. The LM Hugoniot displays a maximum compression of about 6 near $p \sim 0.9$ Mbar, and ultimately converges with the metallic EOS result (the long dashed line in Fig. 3) as x approaches unity. In the limit of infinite temperature, of course, all Hugoniots must asymptotically approach the ideal-gas “compression limit” of $\rho/\rho_0 = 4$, which for our initial state corresponds to a final density of 0.68 g/cm^3 . One can see that in general,

the predictions of the LM model are in good agreement with the experimental data points shown, while those derived from the Sesame database and molecular dynamics calculations are not. Below a pressure of about 0.15 Mbar where dissociation is negligible and deuterium is a molecular fluid, all models agree with the gas-gun data and give essentially the same answer; above this value, though, they begin to differ appreciably. We should mention that some controversy about the LM model has arisen recently as the result of new experiments performed on the Z Accelerator at Sandia National Laboratories [77]. In those experiments, the principal deuterium Hugoniot up to 0.71 Mbar was measured, but so far, the data are in better agreement with the TBMD, GGA-MD, and Sesame predictions than with the LM model.

The LM model can also reproduce fairly accurately *double-shock* Hugoniot measurements of compressed deuterium at pressures up to 6 Mbar, as reported recently by Mostovych *et al.* [27, 28]. In these experiments, a planar, laser-driven shock wave was launched into a deuterium payload that was adjacent to an aluminum “witness plate.” The key idea of the study was to exploit the fact that upon encountering a deuterium/aluminum interface, an initial shock will give rise to two secondary waves: a reflected shock — which will travel backwards into the deuterium and thereby compress it to higher densities and pressures — and a transmitted shock that will propagate into the aluminum. Ascertaining the properties of the doubly-compressed deuterium sample in such an experimental arrangement relies on the fact that the pressures of reflected and transmitted shocks are equal. (This is the so-called impedance matching criterion [23].) Furthermore, since the EOS properties of aluminum are well known [78, 79], the pressure of the transmitted shock can be determined by simply measuring its propagation velocity through the witness plate. Shock propagation velocities in the Mostovych *et al.* experiments were computed from known physical dimensions and time-of-flight measurements recorded on a high-speed streak camera. See Ref. [28] for more specific details on the experimental method used to make these measurements.

It is important to note that the experiments of Mostovych *et al.* differ from most earlier investigations of the EOS of deuterium in that the properties of a *secondary* — and not the principal — Hugoniot curve were investigated. Moreover, these experiments measured the pressure of the reflected shock as a function of the initial shock velocity in the deuterium, and cannot be compared directly with principal Hugoniot measurements in the plane of initial shock pressure and density. By using a simple analytical model for the EOS of aluminum [5],

though, secondary Hugoniot curves can be computed for the various deuterium EOS theories and compared with the data; such a comparison is shown in Fig. 4. One can see that once again, the *ab initio* and Sesame theories do not in general agree with the experimental results, whereas the LM model does. We note that essentially the same conclusion has been reported recently by Militzer *et al.* [39], who also pointed out that a relatively large and seemingly unphysical shift in the specific internal energy of several eV per atom is required to bring the *ab initio* predictions into agreement with the Mostovych *et al.* data and the LM model. We should remark, though, that the agreement between the LM theory and the experimental data in Fig. 4 may be somewhat fortuitous since the validity of LM model at pressures above several Mbar is suspect [44].

An additional comment is warranted here concerning the calculation of the secondary Hugoniot for the LM model shown in Fig. 4. To generate this curve, we found it convenient to construct a table of EOS data for the LM model (available for downloading at the website <http://other.nrl.navy.mil/Preprints>) that could be used to form smooth interpolation functions for the pressure and specific internal energy over a fairly wide range of density and temperature values. Such an interpolation table simplifies the methodology for computing a Hugoniot curve for the LM model in that p and ε are given *directly* as functions of ρ and T . Thus, use of this EOS table makes it unnecessary to solve for d_{min} as an intermediate step; that calculation has already been performed, and the result tabulated along with the data for the pressure and specific internal energy. The bounds of density and temperature values in the table are $0.4 - 3.1 \text{ g/cm}^3$, and $3,000 - 100,000 \text{ K}$, respectively, which is the expected range of validity (approximately) for the LM model.

Let us now turn to a discussion of several important physical quantities, and their variation along the principal Hugoniot curve for the LM model shown in Fig. 3. The first of these is the dissociation fraction x , which was computed using Eq. (8), and is plotted in Fig. 5. The dissociation fraction is a dimensionless quantity that varies monotonically between zero and one, and can be interpreted physically as the ratio of dissociated molecules to the total number of pairs of atoms present in the mixture. Up to a pressure of about 0.2 Mbar, this quantity is essentially zero indicating that the presence of dissociated molecules is negligible, but then increases significantly thereafter. Near the “knee” of the Hugoniot curve in Fig. 3 where $p \simeq 0.9 \text{ Mbar}$, the deuterium fluid is approximately 88% dissociated. One minor shortcoming of the LM model as described here is that the value of x never actually

reaches the limiting value of unity. This is possibly related to the fact that the expression for Z_{vib} in Eq. (17) does not have the correct limiting behavior at high temperatures [61]. Nevertheless, the asymptotic limit of x in the LM model for the chosen initial conditions is actually very close to 1 — about 0.99 — which is quite adequate for our purposes.

Using the LM model, it is instructive to consider the variation along the principal Hugoniot of other physical quantities such as the thermal energy, specific heat, Grüneisen coefficient, and sound speed. All of these quantities can be computed using the Mathematica code in Appendix C, and are plotted in Fig. 6. Figure 6(a) shows a comparison of the thermal energy kT and the Fermi energy

$$\varepsilon_F = \left(\frac{3}{8\pi}\right)^{2/3} \frac{h^2(\rho/m_D)^{2/3}}{2m_e}, \quad (40)$$

where m_e is the mass of an electron. For the range of pressures considered, the condition $kT < \varepsilon_F$ is always satisfied, which implies that the electrons in this system are at least moderately degenerate. Thus, accurate EOS modeling here probably relies more strongly on concepts borrowed from condensed matter theory than traditional high-temperature plasma physics [51]. Figures 6(b) and 6(c) show plots of the specific heat at constant volume

$$c_V = \left(\frac{\partial\varepsilon}{\partial T}\right)_\rho, \quad (41)$$

and the Grüneisen coefficient, Γ , respectively. The general relationship between these two quantities is

$$\Gamma = \frac{1}{\rho c_V} \left(\frac{\partial p}{\partial T}\right)_\rho. \quad (42)$$

The fact that Γ , and hence $(\partial p/\partial T)_\rho$, is slightly negative near a pressure of about 0.5 Mbar is a curious and perhaps serendipitous phenomenological prediction of the LM model; Ross argues that this feature suggests the formation of covalently bonded species in the partially dissociated deuterium fluid [44], although the model does not explicitly attempt to describe such phenomena. (See Ref. [54], though, for an extended version of the LM theory that purportedly models the effects of chainlike structures in shock-compressed liquid deuterium.) Finally, Fig. 6(d) shows a plot of the sound speed

$$c_s = \left[\left(\frac{\partial p}{\partial \rho}\right)_T + \frac{T}{\rho^2 c_V} \left(\frac{\partial p}{\partial T}\right)_\rho^2 \right]^{1/2}, \quad (43)$$

along the Hugoniot. Although the available experimental data is limited, this result is consistent with initial laboratory measurements [80] up to 0.2 Mbar.

IV. SUMMARY AND CONCLUSIONS

In recent years, much attention has been focused on the properties of dense deuterium, mainly as the result of a series of laser-driven, high-pressure Hugoniot measurements [25–28, 34–36]. The LM model proposed by Ross [44] can accurately reproduce these experimental data, while other EOS theories for deuterium cannot [29–33, 38, 40–42]. The LM model is based on the assumption that the thermodynamic properties of deuterium can be described as the composite average of molecular and metallic phases. This *ansatz* possesses the correct limiting behavior for the molecular phase at normal liquid density, and interpolates smoothly to the monatomic-metallic phase at high density. The LM model for deuterium is thought to be applicable at temperatures up to a few electron-volts and pressures of several megabars, where a strongly-coupled degenerate plasma is assumed to exist.

The principal objective of this report has been to provide a detailed reproduction of Ross’ LM model, including an explicit listing of a computer code for computing the principal Hugoniot, and thermodynamic functions such as the specific heat, Grüneisen coefficient, and sound speed. No such self-contained reproduction presently exists in the published literature, and it is anticipated that the information contained herein will be particularly valuable and time conserving to researchers wishing to use the LM model in their study of the properties of compressed deuterium for ICF applications. Although the formulation of the model is straightforward, it nevertheless involves a series of nontrivial computations that are likely challenging for those unfamiliar with EOS modeling theory. While several modifications of the LM model have been proposed to incorporate various physical processes such as electron thermal effects [56], electron-ion screening [55], and the formation of chain-like structures in deuterium [54], we have not attempted to address these phenomena here; rather, we have chosen to focus on reproducing the LM model in its simplest form, including the use of an *ad-hoc* entropic term ($-2.8 NkT$) in the metallic Helmholtz free energy. This term, which is included to crudely model high-order quantum effects that are omitted by the LM model, does not affect the pressure or specific internal energy directly, but does have an appreciable influence on the dissociation fraction. Without it, the “knee” of the principal Hugoniot curve is much less pronounced, and is no longer in agreement with the high-pressure, laser-driven experimental data.

As a final remark, we should point out that considerable controversy still surrounds

the subject of the EOS of deuterium, particularly in light of new Hugoniot data obtained on the Z Machine at Sandia National Laboratory, and reported recently in the literature [77]. Although the Sandia single-shock measurements only extend to pressures of about 0.71 Mbar, they unmistakably show much better agreement with the Sesame database and the *ab initio* molecular dynamics simulations than with the earlier laser-driven data, or the LM model. Undoubtedly, time and further experimentation will be required to resolve this discrepancy.

ACKNOWLEDGMENTS

This work was supported by the U.S. Department of Energy. Useful discussions with Drs. A.N. Mostovych, A.L. Velikovich, and A.J. Schmitt are also acknowledged.

APPENDIX A: MATHEMATICA CODE TO COMPUTE I AND I_η

```
(* ----- Calculation of configuration-free-energy integrals for D2 ----- *)
* ----- *)
* ---> J.W. Bates      U.S. Naval Research Laboratory      May 24, 2001 <--- *)
* ----- *)

This Mathematica code generates the integral, and its derivative with
respect to the packing fraction, appearing in the configurational free
energy for the molecular fluid equation of state of deuterium. See
Eqs. (19) and (30) in this report, and Ross et al. (1983).

----- First, clear all variables used! ----- *)
Clear[third,twothirds,half,No,k,massD2,c,rstar,bohr,hartree,r0,alpha,
      beta,gamma,rc,r1,c1,c2,c3,c4,c6,c8,c9,c10,f,xplus,xminus,
      troot,S,dSeta,L,dLeta,g,dgeta,G,dGeta,fSG,phiSG,phi,impig,
      dimpigeta,HSInteg,dHSIntegeta,etaf,HSIntegTerm,dHSIntegTermeta,
      rho0,do,stmp,l,t,n,x,eta,r,rau,d,rho];

      third = 1/3;
      twothirds = 2/3;
      half = 1/2;

      No = 1.506 * 10+23;      (* # particles per unit mass [g-1] *)
      k = 1.380 * 10-16;      (* Boltzmann's constant [erg/K] *)
      massD2 = 6.690 * 10-24; (* Mass of deuterium molecule [g] *)
      bohr = 0.529;           (* Angstroms PER Bohr radius *)
      hartree = 4.360 * 10-11; (* Equivalent of 1 hartree [erg] *)

(* - Constants required to compute pair potential for deuterium molecules - *)
      alpha = 1.713;          (* Dimensionless . . . . . [-] *)
      beta = 2.961;          (* Has units of . . . . [Angstrom-1] *)
      gamma = 0.01876;      (* Has units of . . . . [Angstrom-2] *)
      c1 = 4.76940;         (* Has units of . . . . [Angstrom-1] *)
      c2 = 2.25457;         (* Has units of . . . . [Angstrom-2] *)
      c3 = 0.955189;        (* Has units of . . . . [Angstrom-3] *)
```

```

c4 = 0.248158;      (* Has units of . . . . [Angstrom^-4] *)
c6 = 0.2666;       (* Has units of . . . . [Angstrom^6] *)
c8 = 1.323;        (* Has units of . . . . [Angstrom^8] *)
c9 = 0.4656;       (* Has units of . . . . [Angstrom^9] *)
c10 = 8.289;       (* Has units of . . . . [Angstrom^10] *)
r0 = 4.365;        (* Has units of . . . . . [Angstrom] *)
rc = 2.55;         (* Has units of . . . . . [Angstrom] *)
r1 = 1.2;          (* Has units of . . . . . [Angstrom] *)

(* ----- Compute hard sphere radial distribution function ----- *)
f[eta_] := (3 + 3*eta - eta^2)/(4*eta^2);
xplus[eta_] := Power[(f[eta] + Sqrt[f[eta]^2 + 1/8]),third];
xminus[eta_] := -Power[(- f[eta] + Sqrt[f[eta]^2 + 1/8]),third];
troot[1,eta_] := 2*eta/(1 - eta)*
  (-1 + xplus[eta]*(Exp[2*1*Pi*I/3]) +
  xminus[eta]/(Exp[2*1*Pi*I/3]));
S[t,eta_] := (1 - eta)^2*(t-troot[0,eta])*(t-troot[1,eta])*
  (t-troot[2,eta]);
dSeta[t,eta_] := -2*(1 - eta)*t^3 + 6*(1-2*eta)*t^2 + 36*eta*t -
  24*eta - 12*(1 + 2*eta);
L[t,eta_] := 12*eta*((1 + eta/2)*t + 1 + 2*eta);
dLeta[t,eta_] := 12*eta*(t/2 + 2) + L[t,eta]/eta;
g[n,x,eta_] := If[x < n, 0,Sum[Residue[
  y/(12*eta*x)*Exp[y*(x - n)]*(L[y,eta]/S[y,eta])^n,
  {y,troot[k,eta]}],{k,0,2,1}]];
dgeta[n,x,eta_] := If[x < n, 0,-g[n,x,eta]/eta + Sum[Residue[
  y/(12*eta*x)*Exp[y*(x - n)]*
  n*((S[y,eta]^n)*L[y,eta]^(n-1)*dLeta[y,eta] -
  (L[y,eta]^n)*S[y,eta]^(n-1)*dSeta[y,eta])/
  (S[y,eta]^(2*n)),{y,troot[k,eta]}],{k,0,2,1}]];
G[x,eta_] := If[x>8,1,Re[Sum[(-1)^(m+1)*g[m,x,eta],{m,1,25}]]];
dGeta[x,eta_] := If[x>10,0,Re[Sum[(-1)^(m+1)*dgeta[m,x,eta],{m,1,25}]]];

```

```

(* ----- Compute intermolecular potential ----- *)
    fSG[r_] := If[r > r0,1,Exp[-(r0/r - 1)^2]];
    phiSG[r_] := hartree*(Exp[alpha - beta*r - gamma*r^2] -
        (c6/r^6 + c8/r^8 - c9/r^9 + c10/r^10)*fSG[r]);
    phi[r_] := If[r<rc,(3.98823*10^-14)*Exp[-c1*(r - rc) -
        c2*(r-rc)^2 - c3*(r-rc)^3 -
        c4*(r-rc)^3*(r-r1)],phiSG[r]];
(* NOTE: Here, the density rho is expressed in units of g/cc, while the *)
(* hard-sphere diameter in expressed in Angstroms *)
    impig[r_,d_,rho_] := 4*Pi*r^2*phi[r]*G[r/d,Pi*d^3*rho/(6*6.69)];
    dimpigeta[r_,d_,rho_] := 4*Pi*r^2*phi[r]*dGeta[r/d,Pi*d^3*rho/(6*6.69)];
(* ----- Integrate product of potential and distribution function ----- *)
    HSInteg[d_,rho_] := NIntegrate[impig[r,d,rho],{r,d,Infinity}]
    dHSIntegeta[d_,rho_] := NIntegrate[dimpigeta[r,d,rho],{r,d,Infinity}]
    etaf[rho_,d_] := Pi*d^3*rho/(6*6.690);
    HSIntegTerm[d_,rho_] := half*(rho/massD2)*No*(10^-24)*HSInteg[d,rho];
dHSIntegTermeta[d_,rho_] := half*(rho/massD2)*No*(10^-24)*
    dHSIntegeta[d,rho];
(* ----- Write table to file ----- *)
    rho0 = 0.40;    (* incremental index = i *)
    d0 = 0.78;    (* incremental index = j *)
    stmp = OpenWrite["lm_molecular_eos_table",FormatType -> OutputForm];
    Do[Write[stmp,(rho0 + (i-1)*0.08),"    ",(d0 + (j-1)*0.08),"    ",
        FortranForm[HSIntegTerm[(d0 + (j-1)*0.08),(rho0 + (i-1)*0.08)]],",    ",
        FortranForm[dHSIntegTermeta[(d0 + (j-1)*0.08),(rho0 + (i-1)*0.08)]]],
        {i,11},{j,15}];
    Close[stmp];

```

APPENDIX B: OUTPUT TABLE OF I AND I_η VALUES

rho (g/cc)	d (A)	I (erg/g)	I_eta (erg/g)
0.40	0.78	3.7442415132351970E11	3.3029390669403570E11
0.40	0.86	3.2882668156982510E11	3.1974768241789440E11
0.40	0.94	2.8718513649605035E11	3.0355855265205130E11
0.40	1.02	2.4970827260916382E11	2.8403655924813250E11
0.40	1.10	2.1634913535586267E11	2.6292011200636307E11
0.40	1.18	1.8689619852376285E11	2.4143449413341058E11
0.40	1.26	1.6104317093999408E11	2.2038796790700046E11
0.40	1.34	1.3843942867953427E11	2.0027470723390628E11
0.40	1.42	1.1872463169250810E11	1.8136856857078168E11
0.40	1.50	1.0155113749617351E11	1.6379798609688068E11
0.40	1.58	8.6596896426510770E10	1.4759762543955930E11
0.40	1.66	7.3572112148382190E10	1.3274440172942296E11
0.40	1.74	6.2221407080970750E10	1.1918139764144803E11
0.40	1.82	5.2323411489707940E10	1.0683539131065990E11
0.40	1.90	4.3688692916181145E10	9.5628168379774020E10
0.48	0.78	4.5048559020172380E11	3.9563250291079443E11
0.48	0.86	3.9611896515021740E11	3.8312179796149550E11
0.48	0.94	3.4651571974036707E11	3.6394624033697070E11
0.48	1.02	3.0191478297947473E11	3.4087504414851465E11
0.48	1.10	2.6225035030795148E11	3.1599040166441974E11
0.48	1.18	2.2726131152662994E11	2.9075836541903470E11
0.48	1.26	1.9657480095197900E11	2.6614347581973755E11
0.48	1.34	1.6976613664719100E11	2.4273132326278146E11
0.48	1.42	1.4640021238680212E11	2.2084100572757916E11
0.48	1.50	1.2605801270854176E11	2.0061585362255203E11
0.48	1.58	1.0835194832044873E11	1.8208667528731537E11

rho (g/cc)	d (A)	I (erg/g)	I_eta (erg/g)
0.48	1.66	9.2933723978202220E10	1.6521495198675030E11
0.48	1.74	7.9496856193590650E10	1.4992285441550848E11
0.48	1.82	6.7776194636512740E10	1.3611370449610541E11
0.48	1.90	5.7545474858108840E10	1.2368616379672395E11
0.56	0.78	5.2693673179759784E11	4.6072869611234784E11
0.56	0.86	4.6391753165911560E11	4.4629759572440310E11
0.56	0.94	4.0647548738210230E11	4.2421245332902580E11
0.56	1.02	3.5487640723134357E11	3.9769996576740630E11
0.56	1.10	3.0903326315321344E11	3.6918446524758720E11
0.56	1.18	2.6863393175681183E11	3.4037181852704290E11
0.56	1.26	2.3323813542681873E11	3.1238266524629580E11
0.56	1.34	2.0234729145705417E11	2.8589437019926495E11
0.56	1.42	1.7545196314642157E11	2.6127205670625946E11
0.56	1.50	1.5206267490752730E11	2.3867552869517917E11
0.56	1.58	1.3172730462256068E11	2.1813408195317902E11
0.56	1.66	1.1404148232802670E11	1.9959756003731384E11
0.56	1.74	9.8648706574791320E10	1.8297101661491455E11
0.56	1.82	8.5242459298171160E10	1.6814268903658994E11
0.56	1.90	7.3562346311468250E10	1.5499275223056550E11
0.64	0.78	6.0377649671729820E11	5.2558151890801280E11
0.64	0.86	5.3222120945572546E11	5.0927238634605880E11
0.64	0.94	4.6706350238872034E11	4.8435162714768195E11
0.64	1.02	4.0859303386922320E11	4.5450133034958795E11
0.64	1.10	3.5669937961982950E11	4.2248611508183580E11
0.64	1.18	3.1101851933733990E11	3.9025050040485310E11
0.64	1.26	2.7104239279886545E11	3.5907128512985583E11
0.64	1.34	2.3619902637471650E11	3.2971851356732056E11
0.64	1.42	2.0590585102560678E11	3.0260508679116095E11

rho (g/cc)	d (A)	I (erg/g)	I_eta (erg/g)
0.64	1.50	1.7960464287340408E11	2.7791007083991860E11
0.64	1.58	1.5678151365849323E11	2.5566538206030127E11
0.64	1.66	1.3697711605471560E11	2.3581509817324628E11
0.64	1.74	1.1978992119617313E11	2.1825612753359616E11
0.64	1.82	1.0487553691549275E11	2.0286621757321870E11
0.64	1.90	9.1944232059936040E10	1.8952214205432294E11
0.72	0.78	6.8100380173464500E11	5.9019002043172960E11
0.72	0.86	6.0102880342954820E11	5.7204352874196560E11
0.72	0.94	5.2827878919323413E11	5.4435830144725586E11
0.72	1.02	4.6306446327072675E11	5.1126940020490356E11
0.72	1.10	4.0525026575877924E11	4.7587932441036020E11
0.72	1.18	3.5441932755472687E11	4.4036999838047020E11
0.72	1.26	3.0999613050288540E11	4.0617431444345740E11
0.72	1.34	2.7133656078493910E11	3.7415612414163617E11
0.72	1.42	2.3778648051056090E11	3.4477819365447350E11
0.72	1.50	2.0872150056234970E11	3.1824219132810730E11
0.72	1.58	1.8356892405841595E11	2.9458751585475415E11
0.72	1.66	1.6181926608746255E11	2.7375888456321634E11
0.72	1.74	1.4303005505145233E11	2.5565253638161655E11
0.72	1.82	1.2682532366076357E11	2.4014753743388223E11
0.72	1.90	1.1289319792388612E11	2.2712637818137952E11
0.80	0.78	7.5861755985517590E11	6.5455326730961800E11
0.80	0.86	6.7033910444190190E11	6.3460842921383560E11
0.80	0.94	5.9012033437024320E11	6.0422711977884070E11
0.80	1.02	5.1829040906495540E11	5.6799452325866980E11
0.80	1.10	4.5468709051196075E11	5.2934825493783136E11
0.80	1.18	3.9884023866756420E11	4.9070590158828595E11
0.80	1.26	3.5010753567356860E11	4.5365612803906525E11

rho (g/cc)	d (A)	I (erg/g)	I_eta (erg/g)
0.80	1.34	3.0777415874673330E11	4.1915745108020260E11
0.80	1.42	2.7111696825115936E11	3.8772438409511414E11
0.80	1.50	2.3944866560325034E11	3.5958411505242480E11
0.80	1.58	2.1214190322399063E11	3.3478761318510406E11
0.80	1.66	1.8864232893092203E11	3.1328528911482526E11
0.80	1.74	1.6847296461755240E11	2.9497813415759250E11
0.80	1.82	1.5123418474460797E11	2.7975145352092834E11
0.80	1.90	1.3660150209230792E11	2.6749191757408408E11
0.88	0.78	8.3661668037669030E11	7.1867034169123830E11
0.88	0.86	7.4015088956260390E11	6.9696454122490270E11
0.88	0.94	6.5258707441399520E11	6.6395282944310970E11
0.88	1.02	5.7427049956088720E11	6.2466725138881310E11
0.88	1.10	5.0501091411604443E11	5.8287727520772340E11
0.88	1.18	4.4428458288351830E11	5.4123387383770264E11
0.88	1.26	3.9138401654283466E11	5.0148057490606550E11
0.88	1.34	3.4552509139526880E11	4.6467083153016920E11
0.88	1.42	3.0591885901765010E11	4.3137180454175287E11
0.88	1.50	2.7181909294541357E11	4.0183763962022736E11
0.88	1.58	2.4254887240849908E11	3.7613238965374890E11
0.88	1.66	2.1751520300991858E11	3.5421281919285940E11
0.88	1.74	1.9621433318458807E11	3.3598254434097015E11
0.88	1.82	1.7823218066155380E11	3.2132235261679270E11
0.88	1.90	1.6324233912043140E11	3.1010025258140600E11
0.96	0.78	9.1500009891103520E11	7.8254034238113990E11
0.96	0.86	8.1046292230160400E11	7.5910936517757170E11
0.96	0.94	7.1567794509185930E11	7.2353028109738830E11
0.96	1.02	6.3100427922295860E11	6.8127831927067520E11
0.96	1.10	5.5622263088172500E11	6.3645098997437710E11

rho (g/cc)	d (A)	I (erg/g)	I_eta (erg/g)
0.96	1.18	4.9075594864849870E11	5.9192966241786630E11
0.96	1.26	4.3383243601227454E11	5.4961114367657260E11
0.96	1.34	3.8460160140510095E11	5.1064295029677686E11
0.96	1.42	3.4221198498955470E11	4.7564410237811900E11
0.96	1.50	3.0586300884651690E11	4.4489446905424146E11
0.96	1.58	2.7483386579938644E11	4.1846805716723730E11
0.96	1.66	2.4849991483612900E11	3.9632035278694434E11
0.96	1.74	2.2633903065595264E11	3.7834042531116170E11
0.96	1.82	2.0793131864374945E11	3.6436849950062380E11
0.96	1.90	1.9295808976022580E11	3.5417033005435200E11
1.04	0.78	9.9376666009435550E11	8.4616238153493690E11
1.04	0.86	8.8127395283580260E11	8.2104044388312480E11
1.04	0.94	7.7939181306880880E11	7.8295442785976970E11
1.04	1.02	6.8849116897282120E11	7.3781864963522030E11
1.04	1.10	6.0832294129474660E11	6.9005427248113070E11
1.04	1.18	5.3825705352112020E11	6.4276938584581770E11
1.04	1.26	4.7745905168683417E11	5.9801123775769070E11
1.04	1.34	4.2501483835940640E11	5.5701911623376220E11
1.04	1.42	3.8001448984253620E11	5.2046095046209937E11
1.04	1.50	3.4160764739068940E11	4.8863680174972500E11
1.04	1.58	3.0903595027950320E11	4.6162058155610680E11
1.04	1.66	2.8165019735134150E11	4.3934647912584924E11
1.04	1.74	2.5891709824668677E11	4.2164827249904650E11
1.04	1.82	2.4041902248873070E11	4.0824344761276530E11
1.04	1.90	2.2584624665246317E11	3.9864255221200244E11
1.12	0.78	1.0729152899169634E12	9.0953558579929910E11
1.12	0.86	9.5258271823021470E11	8.8275536478360560E11
1.12	0.94	8.4372752018756730E11	8.4222032515729080E11

rho (g/cc)	d (A)	I (erg/g)	I_eta (erg/g)
1.12	1.02	7.4673062905837410E11	7.9427935788414160E11
1.12	1.10	6.6131245293406020E11	7.4367227922479030E11
1.12	1.18	5.8679045217074900E11	6.9372930117458500E11
1.12	1.26	5.2226951324984950E11	6.4664420655928850E11
1.12	1.34	4.6677494762569370E11	6.0374372164152990E11
1.12	1.42	4.1934235158043690E11	5.6573863644566590E11
1.12	1.50	3.7907700857114510E11	5.3293836321616210E11
1.12	1.58	3.4518877269325310E11	5.0539732889191956E11
1.12	1.66	3.1701019806838556E11	4.8299030188420090E11
1.12	1.74	2.9400259310372595E11	4.6542283344112890E11
1.12	1.82	2.7575118877441785E11	4.5215021864640280E11
1.12	1.90	2.6194426756178250E11	4.4214010927652030E11
1.20	0.78	1.1524450107253833E12	9.7265909904848950E11
1.20	0.86	1.0243879426536895E12	9.4425175535357630E11
1.20	0.94	9.0868387377776530E11	9.0132312876829830E11
1.20	1.02	8.0572192394250150E11	8.5065179894561070E11
1.20	1.10	7.1519145201220340E11	7.9729047087339380E11
1.20	1.18	6.3635837465529580E11	7.4478609698559800E11
1.20	1.26	5.6826886251590270E11	6.9547345014194240E11
1.20	1.34	5.0989090880900500E11	6.5076050319025770E11
1.20	1.42	4.6021047130351917E11	6.1139071419823050E11
1.20	1.50	4.1829165011006100E11	5.7766610950718400E11
1.20	1.58	3.8331967311850964E11	5.4958934853082806E11
1.20	1.66	3.5461299300721606E11	5.2691707080582060E11
1.20	1.74	3.3162848919604190E11	5.0911787879339280E11
1.20	1.82	3.1394514255548395E11	4.9516076845392770E11
1.20	1.90	3.0121603918033655E11	4.8306397219580770E11

APPENDIX C: MATHEMATICA CODE FOR LM MODEL

```
(* ----- Reproduction of Ross's LM model of dissociating deuterium -----
* ----- *
* --> J.W. Bates      U.S. Naval Research Laboratory      May 21, 2001 <-- *
* ----- *

This Mathematica code generates the principal shock Hugoniot for
deuterium. The approach is based on the work by Ross (1998), and
is known as the linear mixing (LM) model. The LM model is thought
to be applicable at temperature up to a few electron-volts and
several megabars of pressure, where a strongly-coupled degenerate
plasma is assumed to exist.

* ----- *)

(* ----- First, clear all variables used! ----- *)

Clear[half,third,twothirds,Navogadro,No,a0,k,me,massD2,massD,echarge,
      Zdeuterium,Adeuterium,h,hbar,nuD2,ID2,Tnu,Ry,Trot,Dzero,TeV,alpha,
      delta,bconst,cconst,dconst,econst,Znu,fermi,rhonot,Tnot,pnot,epsnot,
      datatable,nlength,confint0table,confint1table,confint0,confint1,etaf,
      epsmol,pmol,FD2conf,Fmol,rs,G,Fmet0,Focp,FEG,fLDA,FZR,Fbcc,Fmet,pmet,
      epsmet,Fegocp,De,q,x,p,eps,hug,dFD2confd,cV,dpT,dprho,cs,grun,dlow,
      dhigh,rholow,rhohigh,Tlow,Thigh,numpts,xytemp,Tvalue,d,rho,T];

      half = 1/2;
      third = 1/3;
      twothirds = 2/3;

(* ----- Specify necessary physical constant in Gaussian cgs units ----- *)

Navogadro      = 6.022 * 10+23;      (* Avogardo's number      [atoms/mole] *)
No              = 1.506 * 10+23;      (* # particles per unit mass [g-1] *)
a0              = 0.529 * 10-08;      (* Bohr radius              [cm] *)
k              = 1.380 * 10-16;      (* Boltzmann's constant    [erg/K] *)
me             = 9.109 * 10-28;      (* Mass of electron        [g] *)
massD2         = 6.690 * 10-24;      (* Mass of deuterium molecule [g] *)
```

```

massD      = 3.345 * 10^-24;      (* Mass of deuterium atom      [g] *)
echarge    = 4.803 * 10^-10;     (* Charge of electron         [esu] *)
Zdeuterium = 1;                  (* Atomic number of deuterium  [-] *)
Adeuterium = 2;                  (* Mass number of deuterium    [-] *)
h          = 6.625 * 10^-27;     (* Planck's constant          [erg*s] *)
hbar       = h/(2*Pi);           (* Planck's constant / 2 pi   [erg*s] *)
nuD2       = 9.155 * 10^+13;     (* D2 vibrational frequency   [s^-1] *)
ID2        = 4.604 * 10^-41;     (* D2 moment of inertia       [g*cm^2] *)
Tnu        = h*nuD2/k;           (* Vibrational temperature     [K] *)
Ry         = 13.6;               (* Ionization energy of D2     [eV] *)
Trot       = (hbar^2)/(2*ID2*k); (* Rotational temperature     [K] *)
Dzero      = -7.585 * 10^-12;    (* Binding energy of D2 molec  [erg] *)
TeV        = 11600.;            (* Conversion factor           [deg/eV] *)
alpha      = 1.602 * 10^-12;     (* Conversion factor           [erg/eV] *)
delta      = -2.8;              (* Coefficient of entropic term [-] *)

(* ----- Specify necessary (dimensionless) constants of OCP model ----- *)
      bconst = 0.95280;
      cconst = 0.18907;
      dconst = -0.81773;
      econst = 2.59;

(* ----- Specify vibrational partition function ----- *)
      Znu[T_] := Exp[-Tnu/(2*T)]/(1 - Exp[-Tnu/T]);

(*      Znu[T_] := Exp[-0.5*Tnu/T]*Sum[Exp[-j*Tnu/T],{j,0,5}]; *)

(* ----- Compute Fermi energy ----- *)
      fermi[rho_] := ((3/(8*Pi))^twothirds)*(h^2/(2*me))*
                    (Navogadro*rho/Adeuterium)^twothirds;

(* ----- Initial state data ----- *)
      rhonot = 0.17;
      Tnot   = 20;
      pnot   = 2*10^-5;
      epsnot = (4.301*10^+10 + No*Dzero - Ry*alpha*2*No)*10^-12;

```

```

(* ----- Read in data table ----- *)
      datatable = ReadList["lm_molecular_eos_table", Number,
                          RecordLists->True];

(* Get length of table *)
      nlength = Dimensions[datatable][[1]];

(* Create data table for interpolating *)
      confint0table = Table[{datatable[[i,2]],datatable[[i,1]],
                          datatable[[i,3]]},{i,nlength}];
      confint1table = Table[{datatable[[i,2]],datatable[[i,1]],
                          datatable[[i,4]]},{i,nlength}];

(* Interpolate *)
      confint0 = Interpolation[confint0table,InterpolationOrder->3];
      confint1 = Interpolation[confint1table,InterpolationOrder->3];

(* ----- Molecular EOS ----- *)
      etaf[d_,rho_] := Pi*d^3*rho/(6*6.690);
      epsmol[d_,rho_,T_] := ((5/2 + Tnu/(2*T) + (Tnu/T)/(Exp[Tnu/T]-1))*No*k*T +
                          confint0[d,rho]) + No*Dzero - Ry*alpha*2*No;
      pmol[d_,rho_,T_] := (rho*No*k*T + rho*etaf[d,rho]*
                          (2*(2 - etaf[d,rho])/((1 - etaf[d,rho])^3) -
                          2*etaf[d,rho]^3 - 2*etaf[d,rho] - 1/2))*No*k*T +
                          rho*confint0[d,rho] + rho*etaf[d,rho]*
                          confint1[d,rho]);
      FD2conf[d_,rho_,T_] := ((4*etaf[d,rho] - 3*etaf[d,rho]^2)/
                          ((1 - etaf[d,rho])^2) - (1/2)*etaf[d,rho]^4 -
                          etaf[d,rho]^2 - etaf[d,rho]/2)*No*k*T +
                          confint0[d,rho];
      Fmol[d_,rho_,T_] := - No*k*T*(
                          Log[((2*Pi*massD2*k*T)^(3/2))/(No*rho*h^3)] + 1 +
                          Log[Znu[T]] + Log[T/(2*Trot)]) + FD2conf[d,rho,T] +
                          No*Dzero - Ry*alpha*2*No;

(* ----- Metallic EOS ----- *)

```

```

rs[rho_] := (3/(4*Pi*Navogadro*Zdeuterium*rho/
(Adeuterium)))^(1/3);
G[rho_,T_] := ((Zdeuterium*charge)^2)/(rs[rho]*k*T);
Fmet0[rho_,T_] := -2*No*k*T*(Log[((2*Pi*massD*k*T)^(3/2))/
(2*No*rho*h^3)] + 1);
Focp[rho_,T_] := 2*No*k*T*
(4*(bconst*(G[rho,T]^(1/4)) -
cconst/(G[rho,T]^(1/4))) +
dconst*Log[G[rho,T]] - econst);
FEG[rho_] := 2*No*Ry*alpha*
(2.21/((rs[rho]/a0)^2) - 0.916/(rs[rho]/a0) -
0.88/((rs[rho]/a0) + 7.8) - 1.792/(rs[rho]/a0));
fLDA[rho_] := 2*No*Ry*alpha*(-0.11382 +
0.003554*rs[rho]/a0 -
0.012707*(rs[rho]/a0)^2);
FZR[rho_] := 2*No*Ry*alpha*
(2.21/((rs[rho]/a0)^2)/(beta/beta0) -
1.792/(rs[rho]/a0));
Fbcc[rho_] := FEG[rho] + fLDA[rho];
Fmet[rho_,T_] := Fmet0[rho,T] + Focp[rho,T] + Fbcc[rho] +
2*No*delta*k*T;
pmet[rho_,T_] := No*(2*rho*k*T*(1 + (1/3)*(bconst*(G[rho,T]^(1/4)) +
cconst/(G[rho,T]^(1/4)) + dconst)) +
2*(rho/3)*Ry*alpha*
(2*2.21/((rs[rho]/a0)^2) - 0.916/(rs[rho]/a0) -
0.88*(rs[rho]/a0)/(((rs[rho]/a0) + 7.8)^2) -
1.792/(rs[rho]/a0) + 2*(0.012707)*
(rs[rho]/a0)^2 - 0.003554*rs[rho]/a0));
epsmet[rho_,T_] := No*(3*k*T + 2*Ry*alpha*
(-1.792/(rs[rho]/a0) + 2.21/((rs[rho]/a0)^2) -
0.916/(rs[rho]/a0) - 0.88/((rs[rho]/a0) + 7.8)) +

```

```

                2*Ry*alpha*(-0.11382 +
                0.003554*rs[rho]/a0 - 0.012707*(rs[rho]/a0)^2) +
                2*k*T*(bconst*(G[rho,T]^(1/4)) +
                cconst/(G[rho,T]^(1/4)) + dconst));
Fegocp[rho_,T_] := Fbcc[rho] + Focp[rho,T] + 2*No*delta*k*T;
(* ----- Compute density- and temperature-dependent dissociation energy ----- *)
De[d_,rho_,T_] := Fegocp[rho,T] - FD2conf[d,rho,T] - No*Dzero +
                2*No*Ry*alpha;
q[d_,rho_,T_] := E*Sqrt[k*T]*massD^(3/2)*Exp[-De[d,rho,T]/(No*k*T)]/
                (16*Sqrt[Pi]*ID2*No*h*rho*Znu[T]);
(* ----- Compute dissociation fraction ----- *)
x[d_,rho_,T_] := Sqrt[q[d,rho,T]/(4 + q[d,rho,T])];
(*      x[d_,rho_,T_] := (q[d,rho,T]/(2*E))*(Sqrt[1 + 4*E/q[d,rho,T]] - 1);      *)
(* ----- Compute total pressure (Mbar) and energy (Mbar*cm^3/g) ----- *)
p[d_,rho_,T_] := (10^-12)*((1 - x[d,rho,T])*pmol[d,rho,T] +
                x[d,rho,T]*pmet[rho,T]);
eps[d_,rho_,T_] := (10^-12)*((1 - x[d,rho,T])*epsmol[d,rho,T] +
                x[d,rho,T]*epsmet[rho,T]);
(* ----- Compute Hugoniot and expression for minimizing FD2conf ----- *)
hug[d_,rho_,T_] := 0.5*(p[d,rho,T] + pnot)*(1/rhonot - 1/rho) +
                epsnot - eps[d,rho,T];
dFD2confd[d_,rho_,T_] := 10^-12*D[FD2conf[w,rho,T],w] /. w -> d;
(* ----- Compute thermodynamic quantities ----- *)
cV[d_,rho_,T_] := D[eps[d,rho,w],w] /. w -> T;
dpT[d_,rho_,T_] := D[p[d,rho,w],w] /. w -> T;
dprho[d_,rho_,T_] := D[p[d,v,T],v] /. v -> rho;
cs[d_,rho_,T_] := 10^6*Sqrt[dprho[d,rho,T] +
                T*(dpT[d,rho,T]^2)/(cV[d,rho,T]*rho^2)];
grun[d_,rho_,T_] := dpT[d,rho,T]/(rho*cV[d,rho,T]);
(* ----- Build array ----- *)
dlow = 1.2;

```

```

    dhigh = 1.45;
    rholow = 0.45;
    rhohigh = 1.15;
    Tlow = 3000;
    Thigh = 100000;
    numpts = 98;

    Array[xytemp, {numpts, 12}];

    Tvalue[j_] := Tlow + (Thigh-Tlow)*(j-1)/(numpts-1);
    Do[{xytemp[j, 1] = FindRoot[{dFD2confd[d, rho, Tvalue[j]] == 0,
                                hug[d, rho, Tvalue[j]] == 0},
                                {d, dlow, dhigh}, {rho, rholow, rhohigh}][[1, 2]],
        xytemp[j, 2] = FindRoot[{dFD2confd[d, rho, Tvalue[j]] == 0,
                                hug[d, rho, Tvalue[j]] == 0},
                                {d, dlow, dhigh}, {rho, rholow, rhohigh}][[2, 2]],
        xytemp[j, 3] = N[Tvalue[j]],
        xytemp[j, 4] = N[p[xytemp[j, 1], xytemp[j, 2], Tvalue[j]]],
        xytemp[j, 5] = N[x[xytemp[j, 1], xytemp[j, 2], Tvalue[j]]],
        xytemp[j, 6] = N[eps[xytemp[j, 1], xytemp[j, 2], Tvalue[j]]],
        xytemp[j, 7] = N[cV[xytemp[j, 1], xytemp[j, 2], Tvalue[j]]],
        xytemp[j, 8] = N[dpT[xytemp[j, 1], xytemp[j, 2], Tvalue[j]]],
        xytemp[j, 9] = N[dprho[xytemp[j, 1], xytemp[j, 2], Tvalue[j]]],
        xytemp[j, 10] = N[grun[xytemp[j, 1], xytemp[j, 2], Tvalue[j]]],
        xytemp[j, 11] = N[fermi[xytemp[j, 2]]],
        xytemp[j, 12] = N[cs[xytemp[j, 1], xytemp[j, 2], Tvalue[j]]],
        {j, 1, numpts}];

(* ----- Write to file ----- *)

stmp = OpenWrite["lm_hugoniot_data", FormatType -> OutputForm];
Do[Write[stmp, " "]];
Do[Write[stmp, "Density", " ", " Temp", " ", " Pressure", " ", " ",
        "Energy", " ", " d ", " ", " x "]];
Do[Write[stmp, "-----", " ", " ----", " ", " -----", " ", " "]];

```

```

"-----" , " " , "-----" , " " , "-----"];
Do[Write[stamp,N[xytemp[j,2],6]," ",
N[xytemp[j,3],6]," ",
N[xytemp[j,4],6]," ",
N[xytemp[j,6],6]," ",
N[xytemp[j,1],6]," ",
N[xytemp[j,5],6]],{j,numpts}];
Close[stamp];

```

APPENDIX D: PRINCIPAL HUGONIOT DATA FOR LM MODEL

rho (g/cc)	T (K)	p (Mbar)	epsilon (Mbar-cc/g)	d (A)	x (-)
0.5090	3000.	0.1367	-7.3938	1.7758	0.00133
0.5564	4000.	0.1852	-7.2833	1.6879	0.01453
0.6299	5000.	0.2504	-7.1239	1.6102	0.06763
0.7471	6000.	0.3449	-6.8780	1.5343	0.20419
0.8849	7000.	0.4567	-6.5764	1.4663	0.41948
0.9827	8000.	0.5493	-6.3255	1.4170	0.60410
1.0348	9000.	0.6186	-6.1411	1.3827	0.71968
1.0607	10000.	0.6748	-5.9950	1.3566	0.79039
1.0729	11000.	0.7241	-5.8693	1.3351	0.83595
1.0775	12000.	0.7695	-5.7554	1.3165	0.86693
1.0777	13000.	0.8124	-5.6490	1.2999	0.88901
1.0754	14000.	0.8537	-5.5476	1.2849	0.90535
1.0715	15000.	0.8938	-5.4497	1.2710	0.91781
1.0666	16000.	0.9331	-5.3546	1.2580	0.92757
1.0611	17000.	0.9717	-5.2616	1.2458	0.93536
1.0553	18000.	1.0097	-5.1703	1.2342	0.94170
1.0493	19000.	1.0473	-5.0803	1.2233	0.94695
1.0432	20000.	1.0845	-4.9916	1.2129	0.95135
1.0372	21000.	1.1214	-4.9039	1.2029	0.95508
1.0312	22000.	1.1580	-4.8171	1.1933	0.95828
1.0253	23000.	1.1944	-4.7311	1.1841	0.96104
1.0195	24000.	1.2306	-4.6458	1.1753	0.96346
1.0138	25000.	1.2665	-4.5611	1.1667	0.96558
1.0083	26000.	1.3023	-4.4771	1.1585	0.96745
1.0030	27000.	1.3379	-4.3936	1.1505	0.96912
0.9977	28000.	1.3733	-4.3107	1.1427	0.97061

rho (g/cc)	T (K)	p (Mbar)	epsilon (Mbar-cc/g)	d (A)	x (-)
0.9927	29000.	1.4086	-4.2282	1.1352	0.97195
0.9878	30000.	1.4437	-4.1461	1.1279	0.97316
0.9830	31000.	1.4787	-4.0645	1.1208	0.97425
0.9784	32000.	1.5136	-3.9833	1.1139	0.97525
0.9739	33000.	1.5484	-3.9024	1.1071	0.97616
0.9695	34000.	1.5831	-3.8219	1.1006	0.97700
0.9653	35000.	1.6176	-3.7418	1.0943	0.97776
0.9612	36000.	1.6521	-3.6619	1.0880	0.97847
0.9572	37000.	1.6864	-3.5824	1.0819	0.97912
0.9533	38000.	1.7207	-3.5032	1.0759	0.97973
0.9496	39000.	1.7549	-3.4242	1.0701	0.98029
0.9459	40000.	1.7890	-3.3455	1.0644	0.98081
0.9424	41000.	1.8230	-3.2671	1.0588	0.98130
0.9390	42000.	1.8569	-3.1889	1.0533	0.98176
0.9356	43000.	1.8908	-3.1110	1.0479	0.98219
0.9323	44000.	1.9245	-3.0333	1.0427	0.98259
0.9291	45000.	1.9582	-2.9558	1.0375	0.98297
0.9261	46000.	1.9919	-2.8786	1.0325	0.98332
0.9231	47000.	2.0254	-2.8015	1.0275	0.98366
0.9201	48000.	2.0589	-2.7247	1.0226	0.98398
0.9173	49000.	2.0924	-2.6480	1.0180	0.98428
0.9145	50000.	2.1257	-2.5716	1.0133	0.98456
0.9118	51000.	2.1590	-2.4953	1.0087	0.98483
0.9092	52000.	2.1923	-2.4192	1.0041	0.98508
0.9066	53000.	2.2255	-2.3433	0.9997	0.98533
0.9041	54000.	2.2586	-2.2676	0.9952	0.98556
0.9017	55000.	2.2917	-2.1920	0.9909	0.98578
0.8993	56000.	2.3247	-2.1166	0.9866	0.98599

rho (g/cc)	T (K)	p (Mbar)	epsilon (Mbar-cc/g)	d (A)	x (-)
0.8970	57000.	2.3577	-2.0413	0.9824	0.98619
0.8947	58000.	2.3906	-1.9662	0.9783	0.98638
0.8925	59000.	2.4235	-1.8913	0.9742	0.98656
0.8903	60000.	2.4563	-1.8165	0.9702	0.98673
0.8882	61000.	2.4891	-1.7418	0.9662	0.98690
0.8862	62000.	2.5218	-1.6673	0.9623	0.98706
0.8841	63000.	2.5545	-1.5929	0.9585	0.98721
0.8822	64000.	2.5872	-1.5186	0.9547	0.98736
0.8802	65000.	2.6198	-1.4445	0.9510	0.98750
0.8783	66000.	2.6523	-1.3705	0.9473	0.98764
0.8765	67000.	2.6848	-1.2966	0.9436	0.98777
0.8747	68000.	2.7173	-1.2229	0.9402	0.98789
0.8729	69000.	2.7497	-1.1492	0.9368	0.98801
0.8711	70000.	2.7821	-1.0757	0.9333	0.98813
0.8694	71000.	2.8145	-1.0023	0.9298	0.98824
0.8678	72000.	2.8468	-0.9290	0.9264	0.98835
0.8661	73000.	2.8790	-0.8558	0.9230	0.98845
0.8645	74000.	2.9113	-0.7827	0.9197	0.98855
0.8629	75000.	2.9435	-0.7097	0.9164	0.98865
0.8614	76000.	2.9757	-0.6369	0.9131	0.98874
0.8599	77000.	3.0078	-0.5641	0.9099	0.98883
0.8584	78000.	3.0399	-0.4914	0.9067	0.98892
0.8569	79000.	3.0719	-0.4188	0.9036	0.98901
0.8555	80000.	3.1040	-0.3463	0.9004	0.98909
0.8541	81000.	3.1360	-0.2739	0.8974	0.98917
0.8527	82000.	3.1679	-0.2016	0.8943	0.98925
0.8514	83000.	3.1999	-0.1294	0.8913	0.98932
0.8500	84000.	3.2318	-0.0573	0.8883	0.98939

rho (g/cc)	T (K)	p (Mbar)	epsilon (Mbar-cc/g)	d (A)	x (-)
-----	-----	-----	-----	-----	-----
0.8487	85000.	3.2636	0.0147	0.8854	0.98946
0.8475	86000.	3.2955	0.0867	0.8825	0.98953
0.8462	87000.	3.3273	0.1586	0.8796	0.98960
0.8450	88000.	3.3591	0.2304	0.8767	0.98966
0.8437	89000.	3.3908	0.3021	0.8739	0.98972
0.8425	90000.	3.4226	0.3737	0.8711	0.98978
0.8414	91000.	3.4543	0.4452	0.8683	0.98984
0.8402	92000.	3.4859	0.5167	0.8656	0.98990
0.8391	93000.	3.5176	0.5881	0.8629	0.98995
0.8379	94000.	3.5492	0.6594	0.8602	0.99001
0.8368	95000.	3.5808	0.7307	0.8575	0.99006
0.8357	96000.	3.6123	0.8018	0.8549	0.99011
0.8347	97000.	3.6439	0.8729	0.8523	0.99016
0.8336	98000.	3.6754	0.9440	0.8497	0.99021
0.8326	99000.	3.7069	1.0149	0.8471	0.99025
0.8316	100000.	3.7384	1.0858	0.8446	0.99030

REFERENCES

- [1] J.D. Lindl, *Inertial Confinement Fusion* (Springer-Verlag, New York, 1998).
- [2] W.B. Hubbard, "Interiors of the giant planets," *Science* **214**, 145-149 (1981).
- [3] M.S. Marley and W.B. Hubbard, "Thermodynamics of dense molecular hydrogen-helium mixtures at high pressure," *Icarus* **73**, 536-544 (1988).
- [4] D. Saumon, W.B. Hubbard, G. Chabrier, and H.M. van Horn, "The role of the molecular-metallic transition of hydrogen in the evolution of Jupiter, Saturn, and brown dwarfs," *Astrophys. J.* **391**, 827-831 (1992).
- [5] S. Eliezer, A. Ghatak, and H. Hora, *An Introduction to Equation of State: Theory and Application* (Cambridge University Press, Cambridge, 1986).
- [6] D.E. Ramaker, L. Kumar, and F.E. Harris, "Exact-exchange crystal Hartree-Fock calculations of molecular and metallic hydrogen and their transitions," *Phys. Rev. Lett.* **34**, 812-814 (1975).
- [7] I. Aviram, S. Goshen, Y. Rosenfeld, and R. Thieberger, "Comments on pressure dissociation of H₂," *J. Chem. Phys.* **65**, 846-847 (1976).
- [8] G. Chabrier, D. Saumon, W.B. Hubbard, and J.I. Lunine, "The molecular-metallic transition of hydrogen and the structure of Jupiter and Saturn," *Astrophys. J.* **391**, 817-826 (1992).
- [9] H. Kitamura and S. Ichimaru, "Metal-insulator transitions in dense hydrogen: equations of state, phase diagrams and interpretation of shock-compression experiments," *J. Phys. Soc. Jpn.* **67**, 950-963 (1998).
- [10] P.C. Souers, *Hydrogen properties for fusion energy* (University of California, Berkeley, 1986).
- [11] J.S. Watson and F.W. Wiffen (eds.), *Radiation Effects and Tritium Technology for Fusion Reactors*, Proceedings of the International Conference on Radiation Effects and Tritium Technology (Gatlinburg, Tenn., 1975).
- [12] R.L. Mills, D.H. Liebenberg, and J.C. Bronson, "Equation of state of fluid T₂ deduced from *P-V-T* and ultrasonic-velocity measurements on H₂ and D₂ to 20 kbar," *J. Appl. Phys.* **49**, 5502-5506 (1978).
- [13] H. Shimizu and T. Kumazama, "Equation of state for fluid hydrogen-isotopes H₂, D₂, and T₂ up to their freezing points at 300K," *J. Chem. Phys.* **78**, 4632-4636 (1983).
- [14] A. Driessen and I.F. Silvera, "The high-pressure equation of state of solid molecular tritium," *J. Low Temp. Phys.* **54**, 565-585 (1984).

- [15] M. Ross, "Matter under extreme conditions of temperature and pressure," *Rep. Prog. Phys.* **48**, 1-52 (1985).
- [16] C.E. Morris, "Shock-wave equation-of-state studies at Los Alamos," *Shock Waves* **1**, 213-222 (1991).
- [17] H.K. Mao and R.J. Hemley, "Ultrahigh-pressure transitions in solid hydrogen," *Rev. Mod. Phys.* **66**, 671-692 (1994).
- [18] P. Loubeyre, R. LeToullec, D. Hausermann, M. Hanfland, R.J. Hemley, H.K. Mao, and L.W. Finger, "X-ray diffraction and equation of state of hydrogen at megabar pressures," *Nature* **383**, 702-704 (1996).
- [19] B.A. Remington, R.P. Drake, H. Takabe, and D. Arnett, "A review of astrophysics experiments on intense lasers," *Phys. Plasmas* **7**, 1641-1652 (2000).
- [20] S.P. Marsh, *LASL Hugoniot Data* (University of California Press, Berkeley, 1980).
- [21] W.J. Nellis, A.C. Mitchell, F.H. Ree, M. Ross, N.C. Holmes, R.J. Trainor, D.J. Erskine, "Equation of state of shock-compressed liquids - carbon-dioxide and air," *J. Chem. Phys.* **95**, 5268-5272 (1991).
- [22] R. Cauble, D.K. Bradley, P.M. Celliers, G.W. Collins, L.B. Da Silva, and S.J. Moon, "Experiments using laser-driven shock waves for EOS and transport measurements," *Contrib. Plasma Phys.* **41**, 239-242 (2001).
- [23] Y.B. Zel'dovich and Y.P. Raizer, *Physics of Shock Waves and High-Temperature Hydrodynamic Phenomena*, Vols. I, II (Academic, New York, 1967).
- [24] L.D. Landau and E.M. Lifshitz, *Fluid Mechanics*, 2nd Ed. (Pergamon, Oxford, 1987).
- [25] L.B. Da Silva, P. Celliers, G.W. Collins, K.S. Budil, N.C. Holmes, T.W. Barbee Jr., B.A. Hammel, J.D. Kilkenny, R.J. Wallace, M. Ross, R. Cauble, A. Ng, and G. Chiu, "Absolute equation of state measurements on shocked liquid deuterium up to 200 GPa (2Mbar)," *Phys. Rev. Lett.* **78**, 483-486 (1997).
- [26] G.W. Collins, L.B. Da Silva, P. Celliers, D.M. Gold, M.E. Foord, R.J. Wallace, A. Ng, S.V. Weber, K.S. Budil, R. Cauble, "Measurements of the equation of state of deuterium at the fluid insulator-metal transition," *Science* **281**, 1178-1181 (1998).
- [27] A.N. Mostovych, Y. Chan, T. Lehecha, A. Schmitt, and J.D. Sethian, "Reflected shock experiments on the equation-of-state properties of liquid deuterium at 100-600 GPa (1-6 Mbars)," *Phys. Rev. Lett.* **85**, 3870-3873 (2000).

- [28] A.N. Mostovych, Y. Chan, T. Lehecha, L. Phillips, A. Schmitt, and J.D. Sethian, “Reflected shock experiments on the equation-of-state properties of liquid deuterium at 100-600 GPa (1-6 Mbar),” *Phys. Plasmas* **8**, 2281-2286 (2001).
- [29] G.I. Kerley, “A theoretical equation of state for deuterium,” Los Alamos Scientific Laboratory Report No. LA-4776, 1972.
- [30] G.I. Kerley, in *Molecular-Based Study of Fluids*, edited by J.M. Haile and G.A. Mansoori (American Chemical Society, Washington, DC, 1983), pp. 107-138.
- [31] D. Saumon and G. Chabrier, “Fluid hydrogen at high density: pressure dissociation,” *Phys. Rev. A* **44**, 5122-5141 (1991).
- [32] D. Saumon and G. Chabrier, “Fluid hydrogen at high density: pressure ionization,” *Phys. Rev. A* **46**, 2084-2100 (1992).
- [33] F.H. Ree, “Phase changes and chemistry at high pressures and temperatures,” in *Shock Waves in Condensed Matter 1987*, edited by S.C. Schmitt and N.C. Holmes (Elsevier, New York, 1988), pp. 125-130.
- [34] N.C. Holmes, M. Ross, and W.J. Nellis, “Temperature measurements and dissociation of shock-compressed liquid deuterium and hydrogen,” *Phys. Rev. B* **52**, 15835-15845 (1995).
- [35] W.J. Nellis, A.C. Mitchell, M. van Thiel, G.J. Devine, R.J. Trainor, and N. Brown, “Equation-of-state data for molecular hydrogen and deuterium at shock pressures in the range 2-76 GPa (20-760 kbar),” *J. Chem. Phys.* **79**, 1480-1486 (1983).
- [36] S.T. Weir, A.C. Mitchell, and W.J. Nellis, “Metallization of fluid molecular hydrogen at 140 GPa (1.4 Mbar),” *Phys. Rev. Lett.* **76**, 1860-1863 (1996).
- [37] C. Pierleoni, D.M. Ceperley, B. Bernu, and W.R. Magro, “Equation of state of the hydrogen plasma by path integral Monte Carlo simulation,” *Phys. Rev. Lett.* **73**, 2145-2149 (1994).
- [38] B. Militzer and D.M. Ceperley, “Path integral Monte Carlo calculation of the deuterium Hugoniot,” *Phys. Rev. Lett.* **85**, 1890-1893 (2000).
- [39] B. Militzer and D.M. Ceperley, “Path integral Monte Carlo simulation of the low-density hydrogen plasma,” *Phys. Rev. E* **63**, 066404/1-10 (2001).
- [40] T.J. Lenosky, J.D. Kress, and L.A. Collins, “Molecular-dynamics modeling of the Hugoniot of shocked liquid deuterium,” *Phys. Rev. B* **56**, 5164-5169 (1997).
- [41] T.J. Lenosky, S.R. Bickham, J.D. Kress, and L.A. Collins, “Density-functional calculation of the Hugoniot of shocked liquid deuterium,” *Phys. Rev. B* **61**, 1-4 (2000).

- [42] G. Galli, R.Q. Hood, A.U. Hazi, and F. Gygi, “*Ab initio* simulations of compressed liquid deuterium,” *Phys. Rev. B* **61**, 909-912 (2000).
- [43] M. Knaup, P.G. Reinhard, and C. Toepffer, “Wave packet molecular dynamics simulations of deuterium in the region of laser shock-wave experiments,” *Contrib. Plasma Phys.* **41**, 159-162 (2001).
- [44] M. Ross, “Linear-mixing model for shock-compressed liquid deuterium,” *Phys. Rev. B* **58**, 669-677 (1998).
- [45] R.W. Zwanzig, “High-temperature equation of state by a perturbation method. I. nonpolar gases,” *J. Chem. Phys.* **22**, 1420-1426 (1954).
- [46] J.A. Barker and D. Henderson, “What is ‘liquid’? Understanding the states of matter,” *Rev. Mod. Phys.* **48**, 587-671 (1976).
- [47] F.H. Ree, “Equilibrium properties of high-density fluids,” *J. Chem. Phys.* **64**, 4601-4605 (1976).
- [48] M. Ross, “A high-density fluid-perturbation theory based on an inverse 12th-power hard-sphere reference system,” *J. Chem. Phys.* **71**, 1567-1571 (1979).
- [49] M. Ross, F.H. Ree, and D.A. Young, “The equation of state of molecular hydrogen at very high density,” *J. Chem. Phys.* **79**, 1487-1494 (1983).
- [50] W.L. Slattery, G.D. Doolen, and H.E. DeWitt, “Improved equation of state for the classical one-component plasma,” *Phys. Rev. A* **21**, 2087-2095 (1980).
- [51] S. Ichimaru, “Strongly coupled plasmas: high-density classical plasmas and degenerate electron liquids,” *Rev. Mod. Phys.* **54**, 1017-1059 (1982).
- [52] F.J. Rogers and D.A. Young, “Validation of the activity expansion method with ultrahigh pressure shock equations of state,” *Phys. Rev. E* **56**, 5876-5883 (1997).
- [53] F.J. Rogers, “New activity expansion calculations for warm dense deuterium,” *Contrib. Plasma Phys.* **41**, 2-3 (2001).
- [54] M. Ross and L.H. Yang, “Effect of chainlike structures on shock-compressed liquid deuterium,” *Phys. Rev. B* **64**, 134210/1-8 (2001).
- [55] P. Arnault, D. Gilles, P. Legend, and F. Perrot, “Equation of state of high density deuterium and hydrogen plasmas: Different attempts to model screening of ion-ion interactions,” *J. Phys. IV (France)* **10**, 291-294 (2000).
- [56] Z. Zinamon and Y. Rosenfeld, “Electron correlation effects and the equation of state of shocked

- liquid deuterium,” *Phys. Rev. Lett.* **81**, 4668-4671 (1998).
- [57] S. Wolfram, *The Mathematica Book*, Fourth Edition (Cambridge University Press, Cambridge, 1999).
- [58] L.E. Reichl, *A Modern Course in Statistical Physics* (John Wiley & Sons, New York, 1998).
- [59] R.C. Tolman, *The Principles of Statistical Mechanics* (Oxford University Press, Oxford, 1938).
- [60] T.L. Hill, *An Introduction to Statistical Thermodynamics* (Dover, New York, 1986).
- [61] J.W. Bates and D.C. Montgomery, “Some numerical studies of exotic shock wave behavior,” *Phys. Fluids* **11**, 462-475 (1999).
- [62] N.F. Carnahan and K.E. Starling, “Equation of state for nonattracting rigid spheres,” *J. Chem. Phys.* **51**, 635-636 (1969).
- [63] M. Ross, “Insulator-metal transition of fluid molecular hydrogen,” *Phys. Rev. B* **54**, R9589-R9591 (1996).
- [64] L.F. Silvera and V.V. Goldman, “The isotropic intermolecular potential for H₂ and D₂ in the solid and gas phases,” *J. Chem. Phys.* **69**, 4209-4213 (1978).
- [65] R.L. Mills, D.H. Liebenberg, and J.C. Bronson, “Equation of state of fluid n-D₂ from *P-V-T* and ultrasonic velocity measurements to 20 kbar,” *J. Chem. Phys.* **68**, 2663-2668 (1978).
- [66] D.A. Young and M. Ross, “Theoretical calculation of thermodynamic properties and melting curves for hydrogen and deuterium,” *J. Chem. Phys.* **74**, 6950-6950 (1981).
- [67] J. van Straaten, R.J. Wijngaarden, and I.F. Silvera, “Low-temperature equation of state of molecular hydrogen and deuterium to 0.37 Mbar: implications for metallic hydrogen,” *Phys. Rev. Lett.* **48**, 97-100 (1982).
- [68] H. Shimizu, E.M. Brody, H.K. Mao, and P.M. Bell, “Brillouin measurements of solid n-H₂ and n-D₂ to 200 kbar at room temperature,” *Phys. Rev. Lett.* **47**, 128-131 (1981).
- [69] M. van Thiel, L.B. Hord, W.H. Gust, A.C. Mitchell, M. D’Addario, K. Boutwell, E. Wilbarger, and B. Barrett, “Shock compression of deuterium to 900 kbar,” *Phys. Earth Planet. Inter.* **9**, 57-77 (1974).
- [70] R.D. Dick and G.I. Kerley, “Shock compression data for liquids. II. Condensed hydrogen and deuterium,” *J. Chem. Phys.* **73**, 5264-5271 (1980).
- [71] M.S. Wertheim, “Exact solution of the Percus-Yevick integral equation for hard spheres,” *Phys. Rev. Lett.* **10**, 321-323 (1963).
- [72] D.L. Goodstein, *States of Matter* (Prentice-Hall, Englewood Cliffs, 1975).

- [73] T.E. Faber, *Theory of Liquid Metals* (Cambridge University Press, Cambridge, 1972).
- [74] N.W. Ashcroft and N.D. Mermin, *Solid State Physics* (Saunders, Fort Worth, 1976).
- [75] T.W. Barbee and M.L. Cohen, "Theoretical study of atomic phases of metallic hydrogen," *Phys. Rev. B* **44**, 11563-11568 (1991).
- [76] W.H. Press, B.P. Flannery, S.A. Teukolsky, and W.T. Vetterling, *Numerical Recipes: The Art of Scientific Computing* (Cambridge University Press, Cambridge, 1987).
- [77] M.D. Knudson, D.L. Hanson, J.E. Bailey, C.A. Hall, and J.R. Asay, "Equation of state measurements in liquid deuterium to 70 GPa," *Phys. Rev. Lett.* **87**, 225501/1-4 (2001).
- [78] L.V. Altshuler, S.B. Kormer, A.A. Bakanova, and R.F. Trunin, "Equation of state for aluminum, copper, and lead in the high pressure region," *Sov. Phys. JETP* **11**, 573-579 (1960).
- [79] A. Mitchell and W. Nellis, "Shock compression of aluminium, copper, and tantalum," *J. Appl. Phys.* **52**, 3363-3374 (1981).
- [80] N.C. Holmes, W.J. Nellis, and M. Ross, "Sound velocities in shocked liquid deuterium," in *Shock Compression of Condensed Matter - 1997*, edited by S.C. Schmitt, D.P. Dandekar, and J.W. Forbes (American Institute of Physics, New York, 1998), pp. 61-64.

Name	Symbol	Value
Number of D_2 molecules per unit mass	N	$1.506 \times 10^{23} \text{ g}^{-1}$
Atomic number of D	Z_D	1
Mass number of D	A_D	2
Mass of D_2 molecule	m_{D_2}	$6.690 \times 10^{-24} \text{ g}$
Mass of D atom	m_D	$3.345 \times 10^{-24} \text{ g}$
Mass of electron	m_e	$9.109 \times 10^{-28} \text{ g}$
Rotational temperature of D_2 molecule	θ_{rot}	87.5 K
Vibrational temperature of D_2 molecule	θ_{vib}	4395 K
Vibrational frequency of D_2 molecule	ν_{D_2}	$9.155 \times 10^{13} \text{ s}^{-1}$
Moment of inertial of D_2 molecule	I_{D_2}	$4.604 \times 10^{-41} \text{ g}\cdot\text{cm}^2$
Binding energy of D_2 molecule	D_0	$-7.585 \times 10^{-12} \text{ erg}$
Binding energy of electron in D atom	E_0	$-2.179 \times 10^{-11} \text{ erg}$
Coefficient of entropic term	δ_e	-2.8
Bohr radius	a_0	$0.529 \times 10^{-8} \text{ cm}$
Boltzmann's constant	k	$1.380 \times 10^{-16} \text{ erg/K}$
Charge of electron	e	$4.803 \times 10^{-10} \text{ esu}$
Planck's constant	h	$6.625 \times 10^{-27} \text{ erg}\cdot\text{s}$
Planck's constant divided by 2π	\hbar	$1.054 \times 10^{-27} \text{ erg}\cdot\text{s}$

TABLE I: Values of physical constants in Gaussian cgs units used in reproducing the LM model.

Parameter	Value	Parameter	Value
α	1.713	c_6	0.2666 \AA^6
β	2.961 \AA^{-1}	c_8	1.323 \AA^8
γ	0.01876 \AA^{-2}	c_9	0.4656 \AA^9
c_1	4.769 \AA^{-1}	c_{10}	8.289 \AA^{10}
c_2	2.255 \AA^{-2}	r_0	4.365 \AA
c_3	0.9552 \AA^{-3}	r_c	2.55 \AA
c_4	0.2482 \AA^{-4}	r_1	1.2 \AA

TABLE II: Values of parameters for computing the deuterium pair potential ϕ with Eqs. (21)-(23).

Note also that $\phi_{SG}(r_c) = 3.988 \times 10^{-14}$ erg.

Initial Quantity	Symbol	Value
density	ρ_0	0.17 g/cm^3
temperature	T_0	20 K
pressure	p_0	2×10^{-5} Mbar
specific internal energy	ε_0	-7.662×10^{12} erg/g

TABLE III: Initial data for the calculation of the principal deuterium Hugoniot.

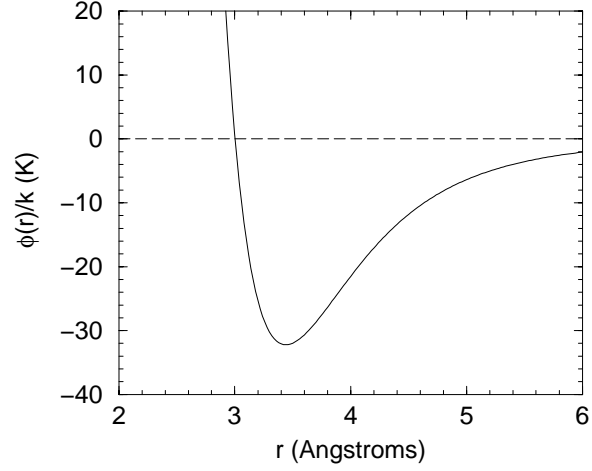


FIG. 1: The softened, Silvera-Goldman pair potential (divided by Boltzmann's constant) for deuterium molecules [64].

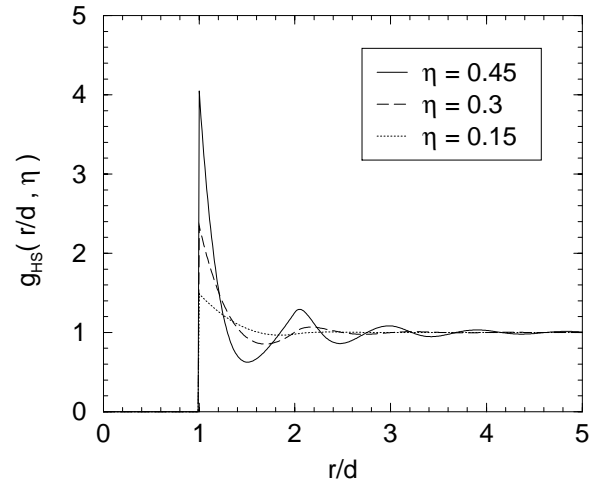


FIG. 2: The pair distribution function for hard spheres [71]. The variables d and η are the hard-sphere diameter and packing fraction, respectively; see Eq. (20).

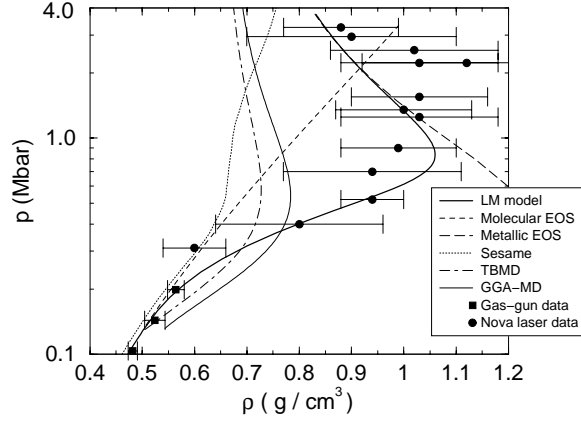


FIG. 3: The principal Hugoniot curve for shocked liquid deuterium based on Ross' LM model. Data from gas-gun and laser-driven shock experiments [26, 35], and results from other EOS models such as Sesame [29], TBMD [40], and GGA-MD [41], are also shown.

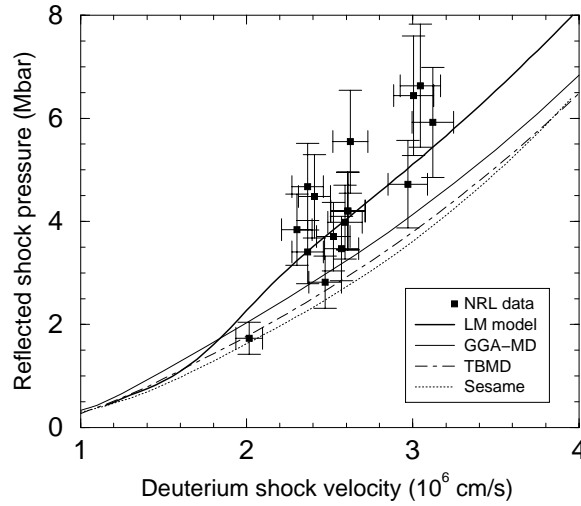


FIG. 4: Comparison of data from double-shock experiments [27, 28] performed at the U.S. Naval Research Laboratory (NRL), and secondary Hugoniot curves derived from the LM [44], Sesame [29], TBMD [40], and GGA-MD [41] EOS models. Here, the pressure of a laser-driven shock wave reflected off an aluminum witness plate is plotted as a function of the initial shock velocity in deuterium.

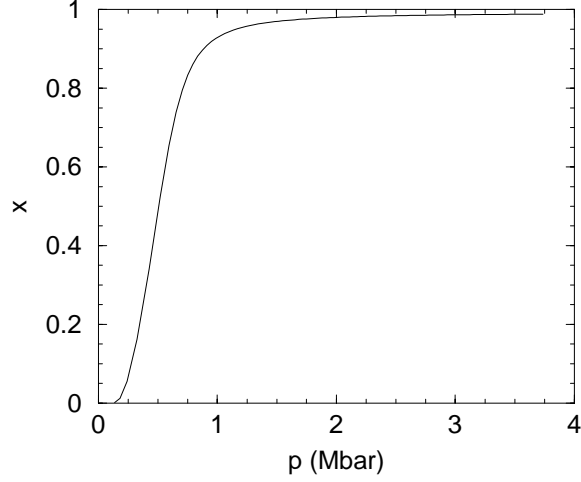


FIG. 5: The dissociation fraction for the LM model along the Hugoniot curve in Fig. 3.

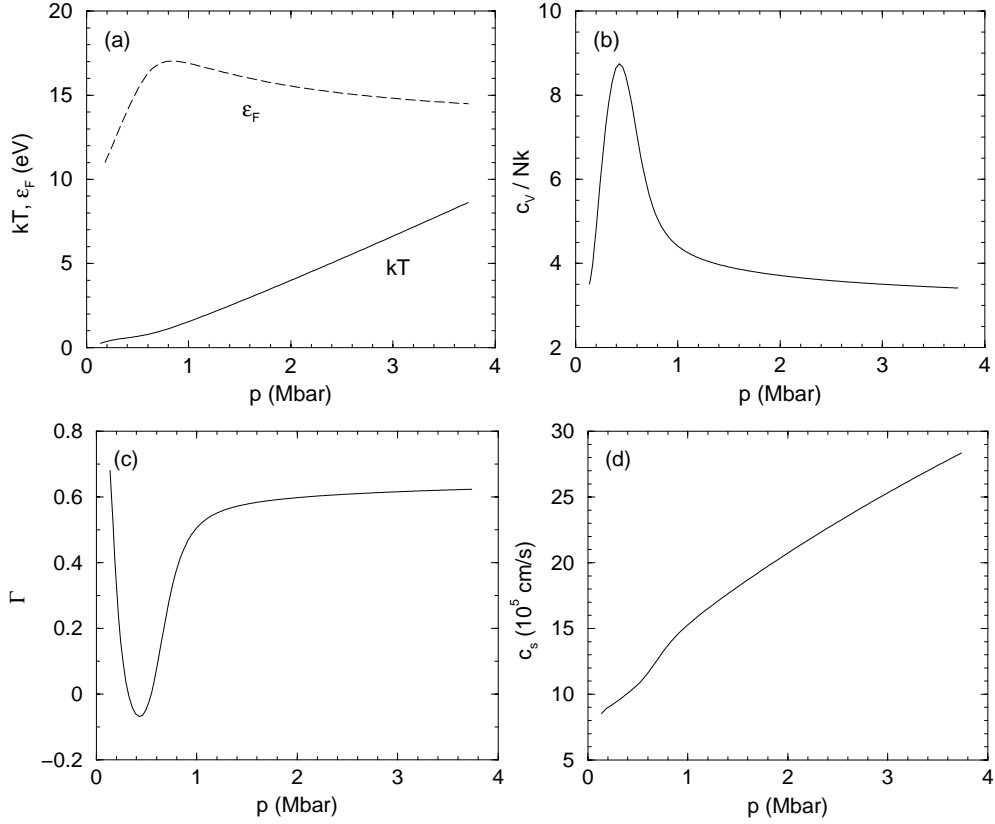


FIG. 6: Variation of (a) the thermal and Fermi energies, (b) specific heat, (c) Grüneisen coefficient, and (d) sound speed along the Hugoniot curve for the LM model in Fig. 3.